THE ROLE OF CHEST CT IN DECIPHERING INTERSTITIAL LUNG INVOLVEMENT: SYSTEMIC SCLEROSIS VERSUS COVID-19

Martina Orlandi[1], Nicholas Landini[2,3], Gianluca Sambataro[4,5], Cosimo Nardi[2], Lorenzo Tofani,[1], Cosimo Bruni, MD[1], Silvia Bellando- Randone[1], Jelena Blagojevic[1], Daniela Melchiorre[1], Michael Hughes[6], Christopher P. Denton[7], Fabrizio Luppi[8], Barbara Ruaro[9], Francesca della Casa[10], Francesca W. Rossi[10], Giacomo De Luca[11], Corrado Campochiaro[11,] Michele Spinicci[12], Lorenzo Zammarchi[12], Sara Tomassetti[13], Antonella Caminati[14], Edoardo Cavigli[15], Marco Albanesi[15], Fabio Melchiorre[16], Stefano Palmucci[17], Virginia Vegni[18], Serena Guiducci[1], Alberto Moggi-Pignone[19], Yannick Allanore[20], Alessandro Bartoloni[12], Marco Confalonieri[9], Lorenzo Dagna[11], Francesco De Cobelli[21], Amato de Paulis[10], Sergio Harari[14,22], Dinesh Khanna[23], Masataka Kuwana[24] , Gloria Taliani[25], Federico Lavorini[13], Vittorio Miele[15], Giovanni Morana[3], Alberto Pesci[8], Carlo Vancheri[4], Stefano Colagrande[2], Marco Matucci-Cerinic[1,11] .

1 Department of Clinical and Experimental Medicine, University of Florence, University of Florence, Division of Rheumatology AOUC, Florence, Italy.
2 Department of Experimental and Clinical Biomedical Sciences, Radiodiagnostic Unit n. 2, University of Florence - AOUC, Largo Brambilla 3, 50134, Florence, Italy.
3 Department of Radiology, Ca' Foncello General Hospital, Piazzale Ospedale, 1, 31100, Treviso, Italy.
4 Regional Referral Centre for Rare Lung Diseases, A. O. U. "Policlinico G. Rodolico – San Marco" Dept. of Clinical and Experimental Medicine, University of Catania, Catania, Italy.
5 Artroreuma S.R.L., Rheumatology Outpatient Clinic Associated with the National Health System, Mascalucia (Catania), Italy.
6 Sheffield Teaching Hospitals NHS Foundation Trust, Royal Hallamshire Hospital, Sheffield, United Kingdom.
7 UCL Division of Medicine Royal Free Hospital, London, United Kingdom.
8 Respiratory Unit, University of Milano-Bicocca, S. Gerardo Hospital, Monza, Italy.
9 Department of Pulmonology, University Hospital of Cattinara, Trieste, Italy.
10 Division of Autoimmune & Allergic Diseases, Department of Translational Medical Sciences. University of Naples Federico II, Napoli, Italy.
11 Unit of Immunology, Rheumatology, Allergy and Rare Diseases, IRCCS San Raffaele Scientific Institute, Vita Salute San Raffaele University, Milan, Italy.
12 Department of Experimental and Clinical Medicine, University of Florence, and Infectious and Tropical Diseases Unit, AOUC, Florence, Italy.
13 Department of Clinical and Experimental Medicine, University of Florence, Florence, Italy.
14 U.O. di Pneumologia, Ospedale San Giuseppe MultiMedica, IRCCS.
15 SOD Radiodiagnostica Emergenza-Urgenza, AOU Careggi, Florence, Italy.
16 Department of Radiology Sant'Andrea Hospital Vercelli, ASLVC Italy.
17 Radiodiagnostic and Radiotherapy Unit, Department of Medical Surgical Sciences and Advanced Technologies "GF Ingrassia", University of Catania, Italy.
18 Radiology Unit, Rugani Hospital, Siena, Italy.
19 Department of Experimental and Clinical Medicine, AOU Careggi Hospital, University of Florence Medical School, Florence, Italy.

[20] Department of Rheumatology A, Descartes University, APHP, Cochin Hospital, Paris, France.
[21] Department of Radiology IRCCS San Raffaele Scientific Institute, Vita-Salute San Raffaele University, Milan, Italy.
[22] Department of Clinical Sciences and Community Health, Università degli Studi di Milano, Italy.
[23] Department of Medicine, University of Michigan, Ann Arbor, MI, USA.
[24] Department of Allergy and Rheumatology, Nippon Medical School Graduate School of Medicine, Tokyo, Japan.
[25] Department of Translational and Precision Medicine, Sapienza University, Rome, Italy.

CORRESPONDING AUTHOR

Martina Orlandi
Department of Clinical and Experimental Medicine, University of Florence, & Department of Geriatric Medicine, Division of Rheumatology AOUC, Florence, Italy.
Padiglione 28c Ponte Nuovo, piano 1. Via delle Oblate, 4, Firenze
Tel. 055 794 7066
ORCID ID: 0000-0001-6784-2235
martina.orlandi@unifi.it

ABSTRACT

Objective: To identify the main computed tomography (CT) features that may help distinguishing a progression of interstitial lung disease (ILD) secondary to Systemic sclerosis (SSc) from COVID-19 pneumonia.

Methods: This multicentric study included 22 international readers divided in the radiologist group (RAD) and non-radiologist group (nRAD). A total of 99 patients, 52 with COVID-19 and 47 with SSc-ILD, were included in the study.

Results: Fibrosis inside focal ground glass opacities (GGO) in the upper lobes; fibrosis in the lower lobe GGO; reticulations in lower lobes (especially if bilateral and symmetrical or associated with signs of fibrosis) were the CT features most frequently associated with SSc-ILD. The CT features most frequently associated with COVID- 19 pneumonia were: consolidation (CONS) in the lower lobes, CONS with peripheral (both central/peripheral or patchy distributions), anterior and posterior CONS and rounded-shaped GGOs in the lower lobes. After multivariate analysis, the presence of CONS in the lower lobes ($p < 0.0001$) and signs of fibrosis in GGO in the lower lobes ($p < 0.0001$) remained independently associated with COVID-19 pneumonia or SSc-ILD, respectively. A predictive score was created which resulted positively associated with the COVID-19 diagnosis (96.1% sensitivity and 83.3% specificity).

Conclusion: The CT differential diagnosis between COVID-19 pneumonia and SSc-ILD is possible through the combination the proposed score and the radiologic expertise. The presence of consolidation in the lower lobes may suggest a COVID-19 pneumonia while the presence of fibrosis inside GGO may indicate a SSc-ILD.

Keywords: COVID-19, COVID-19 pneumonia, interstitial lung disease, systemic sclerosis, lung CT scan.

Key messages:

CT differential diagnosis between COVID-19 pneumonia and interstitial lung disease secondary to Systemic sclerosis (SSc-ILD) is possible.

The presence of fibrosis inside ground glass opacities may indicate a SSc-ILD.

The presence of consolidation in the lower lobes may indicate a COVID-19 infection.

INTRODUCTION

The COVID-19 pandemic is characterised by an interstitial pneumonia and vascular damage that may lead to a severe and sometimes fatal outcome [1]. In systemic sclerosis (SSc), interstitial lung disease (ILD) is one of the main features of the disease [2-3] During the last few months, it has clearly emerged that COVID-19 and SSc may share similar radiological features [4]. Recently we raised the question of whether, in SSc, the onset of bilateral and subpleural lung alterations in chest HRCT were due to the rapid onset, acute exacerbation or progression of SSc-ILD or the overlap of COVID19 pneumonia [5]. In both diseases, the presence of bilateral and subpleural ground glass opacities (GGO), with or without consolidations, are the most frequent radiological alterations [6]. In SSc-ILD, the most common radiological pattern is non-specific interstitial pneumonia (NSIP) with peripheral, bibasilar distribution of GGO and a lower proportion of reticulation, while usual interstitial pneumonia (UIP) may be present in up to a third of patients [7-12]. In COVID-19 patients, ILD pneumonia is characterized by bilateral GGO, evolving into consolidations, with a peripheral distribution mostly involving lower lung areas [13]. Although none of the CT features of COVID-19 seems to be specific, lung CT has a fundamental role in the diagnostic algorithm for COVID-19 pneumonia. Recently, the Radiological Society of North America proposed a radiologic classification of COVID19 pneumonia which focused the attention on the fact that also a typical COVID-19 CT pattern may be found in other ILDs, such as that found in connective tissue diseases [14]. Therefore, the differential diagnosis between the two diseases is a real challenge in practice. Drawing parallels between SSc-ILD and COVID-19 offers potential insight into both diseases as well as being of practical clinical relevance.

Considering this background, the primary goal of our study was to identify the main CT features of COVID-19 pneumonia and SSc-ILD that may help distinguishing both diseases. The secondary endpoint was to evaluate the ability and concordance between radiologists and non-radiologists/clinicians, on chest CT, in differentiating SSc-ILD from COVID-19 pneumonia, based on their CT expertise reading.

MATERIALS AND METHODS

Patients and images selection

COVID-19 pneumonia and SSc-ILD patients were eligible for the study. The COVID-19 group included patients with both positive by RT-PCR for COVID-19 and available chest CT imaging, performed within two weeks since the PT-PCR diagnosis. COVID-19 patients were retrospectively recruited from Florence and Treviso hospital from March 1 to May 30, 2020. The COVID CTs were acquired at the hospital admission or within 3 days, for functional deterioration. For each COVID-19 patient, we tried to identify a SSc-ILD gender- and age-matched patient fulfilling the 2013 ACR/EULAR criteria for SSc [15] with CT images acquired before 2019. The identified CT scans were directly downloaded from the hospital Picture Archiving and Communications Systems.
All CT scans had slice thickness ranging from 1.0 to 1.5 mm. All CT were scanned at full Inspirations in supine position. Some additional prone CT were acquired in SSc patients, as it may be occasionally performed for ILD assessment [16]. However, these additional CT were excluded from the analysis to avoid any lecture bias, since CT in COVID patients were acquired only in supine position. Images were anonymized and randomized. Patients were identified with an alpha numeric code, in the respect of the privacy rules. The CT scans were saved as DICOM files, sent to the readers through a password-protected sharing platform (Dropbox business). A free DICOM viewer (Radiant DICOM Viewer 2020.1) was also suggested.

Methods and Study design

This retrospective, observational, multicentric, international study was approved by the Institutional Ethics Committee of Florence Careggi hospital (protocol number 17104_oss).

Phase I – the gold standard

Two chest radiologists (NL and EC) with more than 5 years' experience in chest imaging evaluated all CTs: disagreements were solved by a senior chest radiologist with more than 10 years of experience (SC). These evaluations were considered as the gold standard for analysis of the correctness and definition of the predictive capacity of the various CT features elements.

Phase II – Image evaluation

This multicentric study included 22 international readers (NL, EC, MA, FM, SP, VV, FDC, GS, CB, SBR, JB, MH, CD, FL, BR, FDC, GDL, LZ, MS, ST, AC), including radiologists (RAD) and non-radiologists (nRAD). The RAD group included 7 radiologists of whom 4 chest radiologists, with at least more than 5 years of experience. The non-RAD group included 15 specialists, including 6 rheumatologists, 3 immunologists, 2 infectious disease specialists, 4 pulmonologists. Detailed information about reader's medical speciality, location of practice, SSc specific training, years of practice, COVID-19 specific training are shown in Supplementary Data S1, available at *Rheumatology* online. Each reader reviewed the images of all patients using Picture Archiving and Communications Systems independently and was blinded to diagnosis, laboratory assay results and demographic information including patient name, hospital of origin of the CTs and date of CT examination.

Image analysis

Each reader was asked to fill an electronic database giving single (i.e. yes / no) or multiple (i.e. mostly anterior, mostly posterior / no prevalence) answers. The definition of all CT lesions and

anatomical references requested in the assessment follows the definitions of the Fleischner society [17,18] and are available in Supplementary Data S2, available at *Rheumatology* online.
CT evaluation was performed at three different levels of detail in order to reach the study's objectives: a first basic level of analysis, common for RAD and nRAD, a second advanced level, specific only for RAD and a third deeper analysis, made by the 4 chest radiologists only, as follows.
The 1st level included the analysis of 56 CT features. CT images were assessed for presence/absence of lung disease, as well as for side (monolateral/bilateral-asymmetric/bilateral-symmetric), prevalent distribution (anterior/posterior/no prevalence, central/peripheral/no prevalence/patchy). Parenchymal lesions assessment was also performed with the same variables, for upper and lower zones. The CT lesions were categorised as: consolidations (CONS), GGO, crazy paving (CP), reticulations (RET) and honey combing (HC). As regards the whole disease, the prevalent localisation (upper/lower/no prevalence), involved lobes and the most extended lesion (CONS, GGO, CP, RET or HC) were also assessed. Air bronchogram inside CONS (always present/not always present/never present), were analysed, too. Lastly, pleural effusion, pericardial effusion, lymphadenopathy and oesophagus dilatation were assessed in terms of absence/presence.
The 2nd level included 14 additional CT features: presence/absence of aspects resembling organizing pneumonia in CONS, as well as signs of fibrosis (defined by architectural distortions or bronchiectasis) in CONS, GGO and RET, finally pleural thickenings in the whole lung fields.
The 3rd level assessed other 8 CT features: disease pattern (monofocal/multifocal/diffuse/focal and diffuse or white lung), GGO pattern (focal, diffuse or both) presence/absence of rounded GGO and presence /absence of fibrosis inside focal GGO. (Supplementary Figure S1, available at *Rheumatology* online).
Each reader, finally, was invited to propose a diagnosis of COVID-19 pneumonia or SSc-ILD.

Statistical analysis and score derivation

Each categorical variable was described as absolute and relative frequencies for each category stratified by diagnosis. In order to evaluate the interreader agreement Cohen's Kappa (K) adjusted for multiple readers and its 95% confidence interval were used. A $K \geq 0.4$, 0.6, 0.8 was considered discrete, good and excellent, respectively. To assess the association between each CT feature and the diagnosis a simple logistic regression model was used and OR and its 95% confidence interval were reported. According to the presence of association the predictive capability was described by AUROC and its 95% confidence interval. An AUROC ≥ 0.8 was considered good while ≥ 0.9, excellent. In order to reach the best predictive performance with the most economical model a multiple logistic regression model with backward selection method for CT features with excellent predictive capability and good interreader agreement was used. According to the multiple logistic model results a score weighted using log (OR) of each selected CT feature was created. Using the AUROC a cut-off was selected, and its sensibility, specificity, positive predictive value and negative predictive value were reported. No external validation of the score cut-off was performed. The significant level was set to 5% for each analysis. Once obtained the results from the RAD analysis, we compared them with the reference results in order to evaluate which could be the features with significantly discriminating capability and subsequently we validated this with a regression model and with multivariate analysis. Lastly, we tried to obtain an incremental score positively associated with the COVID-19 diagnosis**.**

RESULTS

A total of 99 patients were included in this study: 52 COVID-19 pneumonia patients and 47 SSc-ILD patients. Mean age was 62.4 (±7) and 60.3 (±6) in COVID-19 and SSc-ILD, respectively, with 19 female patients in the SSc-ILD group and 23 in the COVID-19 group.

1.Interreader agreement

The full detailed results about interreader agreement are available in Supplementary Table S1, available at *Rheumatology* online.

1.1 nRAD interreader agreement

The interreader agreement for the evaluation of all the different items was scarce (0.03-0.36). For this reason, this was not considered relevant for the subsequent evaluations. (Supplementary Table S2, available at *Rheumatology* online).

1.2.RAD interreader agreement

In the RADs group, a discrete-good agreement for 47% of the items (33/70) was detected, with a K Cohen from 0.60 to 0.71. When readers were divided according to the skill concerning chest CT, chest RAD showed a better concordance for the items considered 68.4% (52/76), and the K Cohen between non-chest RAD and chest RAD was significantly different ($p < 0.05$) in 51.4% of items (36/70), and in 35.71% of variables (25/70) p-values was < 0.005 (Supplementary Table S1, available at *Rheumatology* online). Considering chest RAD, the agreement was good, with a K Cohen value from 0.62 e to 0.74. Out of 70 CT features proposed to RAD readers for analysis, 39 showed a discrete and 33 a good intrareader agreement: only the latter were considered suitable for subsequent evaluations.

2. Diagnostic performance

2.1 nRAD diagnostic performance

The nRAD made a correct diagnosis (COVID-19 pneumonia or SSc) in 77.5% (IC95%: 75.13-79.74). In particular, a correct diagnosis was achieved in 75.95% COVID-19 patients (499/657 evaluations) and 78.95% SSc patients (510/646 evaluations) (Table 1).

2.2 RAD diagnostic performance

The RAD made a correct diagnosis in 83.92% of cases (80.95%-86.59% CI): 86.61% COVID-19 pneumonia patients and 81.08% SSc subjects (Table 1). Diagnostic performance between nRAD and RAD were statistically different ($p = 0.0008$) (Table 1). The correct diagnosis was done (all, COVID-19 pneumonia or SSc-ILD) respectively: chest RAD group, in 86.53% (83.18% -89.43% CI); 88.40% (221/250); 84.58% (67/93) patients; non-chest RAD group in 72.04% (70.77-83.01 % CI); 82.18% (82/101); 72.04% (203/240) patients. A significant difference between chest and non-chest RAD was found ($p = 0.0034$) (Table 1).

3. Diagnostic predictive value CT features

Given the scarce concordance in nRAD group and the significant difference in concordance between chest-RAD and non-chest-RAD, only those parameters for which radiologists had shown good or excellent concordance (Table 2) were considered as possible discriminating parameters and so accepted as relevant for differential diagnosis between COVID-19 and SSc-ILD. The complete CT features predictive values were reported (Supplementary Table S2, available at *Rheumatology* online).

4. Discriminating CT features

We identified main CT features of COVID-19 pneumonia and SSc-ILD, considering only those showing good concordance and good/excellent discriminating capability. CT features most likely associated with SSc-ILD were: fibrosis inside focal GGO in the upper lobes; fibrosis in lower lobe GGO; RET in lower lobes, especially if bilateral/symmetrical or with signs of fibrosis; while those associated with COVID-19 pneumonia were: CONS in the lower lobes; CONS with peripheral, both central/peripheral or patchy distributions; both anterior and posterior CONS; rounded-shaped GGOs in the lower lobes. (Table 2).

5. Model derivation

A multivariate regression model was developed to select variables independently related to the diagnosis of COVID-19 pneumonia. Out of 99 patients involved, the 5 most significant associated predictors were, according to clinical decision, feasibility, good reproducibility and good/excellent predictive ability: CONS in lower zone, rounded GGO in lower zone (both predictive for COVID-19 pneumonia), fibrosis in GGO in lower zone, inside focal GGO fibrosis in the upper zone and lower lobes RET (all predictive for SSc-ILD). Otherwise, only lower lobes CONS ($p < 0.0001$) and signs of fibrosis in GGO lower lobes ($p < 0.0001$) resulted as independent predictors (Table 3). On this basis we proposed a score which might identify the CT associated with the COVID-19 diagnosis (OR: 2.67, IC95%: 1.76-4.07), as follows: CONS: 4 points if presents, 0 if absent; GGO: 5 points if present without fibrosis, 0 if present with fibrosis, 3 if absent.

This score showed an excellent predictive capability, with area under the ROC curve of 0.97 (0.94-1.00 CI) (Table 3 and Supplementary Figure 2, available at Rheumatology online). The score cut off was 4 (chosen in order to guarantee greater sensitivity and specificity to the score) and, if ≥ 4, it is associated with a diagnosis of COVID-19. The score diagnostic performance was 96.1% sensitivity (86.5% -99.5% CI) and 83.3% specificity (69.8% -92.5% CI). The negative predictive value was 95.2% (83.8% -99.4% CI), and the positive predictive value was 86.0% (74.2% -93.7% CI).

DISCUSSION

Our data show, as far as we know for the first time, that a differential diagnosis between COVID-19 and SSc-ILD is possible in practice, employing the CT images: the presence of consolidations and fibrosis inside GGO in the lower lobes, are independent CT diagnostic feature for COVID-19 pneumonia and SSc-ILD diagnosis, respectively (Figure 1).

This differential diagnosis represents a new challenge for clinicians and radiologists [19,20]. Recently, the RSNA [14] identified 3 CT patterns of COVID19 pneumonia: peripheral and bilateral GGO, regardless the coexistence of consolidation; CP or multifocal rounded GGO, regardless the coexistence of consolidation or CP; findings of organizing pneumonia. However, these features of COVID-19 pneumonia can also be found in other lung diseases, such as those related to connective tissue diseases [7,14]. The most common radiological pattern in SSc-ILD is NSIP with peripheral, bibasilar distribution of GGO and a lower proportion of coarse reticulation [4,8-12]. On top of radiological similarities, the clinical presentation is similar in both diseases, as well. Otherwise, fever and rapid onset shortness of breath are peculiar for COVID-19 pneumonia [21-23]. However, suspicion for a SARS-CoV-2 infection in symptomatic SSc patients should be raised also in the absence of fever, since in most of these patients, fever is absent due to treatment with immunosuppressors. So, in the COVID-19 era, it was hard for clinicians to provide an accurate diagnosis and lung CT has played a pivotal role in the creation of a diagnostic algorithm for patients with suspected COVID-19 pneumonia and a predictive CT score may be useful. We evaluated the main CT features related to COVID-19 pneumonia and SSc-ILD, trying to identify the specific lesions that could help in differential diagnosis. We decided on a multi-step evaluation of CT alterations considering the relative expertise of all the readers, to highlight the relevance of a specific expertise in chest CT for imaging evaluation. Surprisingly, we found low agreement among chest RAD in distinguishing between prevalent anterior/posterior (or no prevalence) distribution of lung disease and of lower zones GGO, regardless of the clear anatomic landmarks. This may suggest that the presence of more than one alteration may produce confusion in the interpretation of the general disease distribution. In fact, all the CT features, considered one-by-one, obtained a higher agreement on both lung zones for anterior-posterior distribution, except for lower zones GGO. In SSc-ILD, GGO can be considered either inflammatory or fibrotic, while RET is usually interpreted as a fibrotic alteration [24]. Thus, we believe that GGO could have been occasionally interpreted as thin RET, and vice versa. This can explain the low agreement of RET presence in upper zones, where fibrotic fine RET may be less represented and considered as GGO. Following the same rationale, CP, defined as GGO superimposed on RET, may suffer for different evaluation in lower zones, where fibrotic alterations can be more pronounced and all considered as RET, instead of CP. The definition of multifocal and diffuse pattern (Supplementary Figure 1, available at *Rheumatology* online) we proposed, as well as the recent identification of vessel thickening as a feature of COVID-19 pneumonia, may have partially caused the low agreement for upper zones GGO pattern and vessel thickening.

On the upper zones, where lung alterations may have more frequently a patchy-irregular distribution, the interpretation between focal and diffuse disease may represent an additional challenge. In fact, GGO may have blurred margins, making hard to define shape and dimensions. This can justify the lower agreement in GGO pattern assessment in upper zones. Moreover, HC showed a low agreement on upper fields, as expected, since HC and paraseptal emphysema are in differential diagnosis and may be misinterpreted (Supplementary Figure 3, available at *Rheumatology* online) [25]. It should be noted that the only 2 cases of SSc ILD and COVID-19 pneumonia were

misdiagnosed by most of nRAD, RAD and chest RAD readers (Figure 2), while, in some subjects the coexistence of both diseases was wrongly suggested by chest RAD. Hence, regarding the RSNA statement [14], we can suppose that the radiologic differential diagnosis is reliable on "pure" lung disease. However, in the latter environment, where there are no clinical doubts between COVID-19 and SSc-ILD, the relevance of CT evaluation in differential diagnosis is less significant, becoming on the contrary, relevant in the identification of the lung disease in COVID infected SSc patients. This is confirmed by our results, and the only aspects that may help in differential diagnosis are consolidation for COVID-19 pneumonia is (Supplementary Figure 4, available at *Rheumatology* online), and fibrosis inside GGO for SSc-ILD (Figure 3). However, consolidations can be absent, especially during the early phase of COVID-19, when a clinical decision may be relevant and GGO is the only main CT feature and a prompt therapy is mandatory. In fact, consolidations were absent in the only subject with coexistence of both disease and few readers made the right diagnosis. This is in line with the few reports present in literature. Cheng et al. [25] observed a COVID-19 pneumonia superimposed on SSc-ILD, with GGO as main manifestations, suggesting a specific care should be used when only GGO is present. In fact, though associated signs of fibrosis may be suggestive for SSc-ILD alone, GGO without fibrosis may potentially represent both diseases. On the other hand, Mariano et al. [26] made a diagnosis of COVID-19 pneumonia on SSc-ILD thanks to the presence of a consolidation superimposed on a UIP pattern in the right lower lobe. Fibrosis in focal GGO in upper zones and RET in lower zones did not result as independent predictor of SSc-ILD, as well as rounded GGO in lower zones for COVID-19 pneumonia (Supplementary Figure 5, available at *Rheumatology* online). In fact, in both diseases the absence of fibrosis in focal alteration as well as lower rounded GGO may be encountered. Thus, on an SSc-ILD background, the appearance of rounded GGO may raise the suspicion of a COVID-19 overlapping on SSc-ILD. This is because fibrotic alterations are not present during the acute phase of COVID-19 pneumonia and could be referred only to SSc-ILD (Figure 3), though we cannot exclude that an acute focal manifestation of COVID-19 pneumonia may appear over focal signs of fibrosis. Furthermore, RET are less frequent in COVID-19 pneumonia (Figure 1).

The two principal items (presence of CONS and presence of GGO without fibrosis (Figure 3) in the lower lobes) were included in a predictive score positively associated with the COVID-19 diagnosis (Figure 1), as follows: *high risk* for COVID-19 pneumonia (5-9 points); *probable overlap* COVID-19 pneumonia in SSc-ILD (4 points); *low risk* for COVID-19 pneumonia (0-3 points).

The score showed an excellent diagnostic accuracy with high sensibility and specificity (Supplementary Figure 2, available at *Rheumatology* online) and could therefore be useful in the clinical routine. However, we recommend considering that GGO without fibrosis may be expression of non-fibrotic NSIP. We strongly suggest to consider the presence of both consolidations and non-fibrotic GGO as signs of COVID-19 pneumonia alone only in presence of other suggestive signs (i.e. rounded shape) and absence of typical SSc-ILD abnormalities (i.e. RET).

The strength of this study is the number of patients that were examined, and the high number of readers and of the considered variables. However, it is important to consider that our aim was not to compare the two patterns in order to find the main features that may then help differentiating the two diseases when superimposed. In this work, only a few cases of COVID-19 superimposed on SSc-ILD were analysed, while COVID-19 and SSc ILD CT images at different stages of the diseases with diverse disease duration and ILD stage were studied.

In conclusion, our study shows that the CT differential diagnosis between COVID-19 pneumonia and SSc-ILD might be successfully achieved in practice. This could be performed also by the

rheumatologist but a specific expert evaluation of a radiologist is always recommended, in particular if an overlap of both diseases is suspected.

Our results, and in particular the presence of consolidations in the lower lobes and of fibrosis inside GGO, may help in differentiating the diseases and drive the physician toward an early diagnosis either of SSc-ILD progression or of an overlap of COVID-19 in SSc-ILD. In the future, our results should be confirmed on a much larger cohort of patients where both diseases coexist.

Contributors

MO, MMC, SG, SC and AMP were involved in the study design. MO, NL, MMC, EC, VV and GC decided the methodology. NL, GS, CB, SBR, JB, DM, MH, CPD, FL, BR, FDC, GDL, MS, LZ, ST, AC, EC, MA, FM, SP, VV, GC, FDC, CV were CTs readers. MO, NL, CN made data collection. LT, MO and NL made statistical analysis.MO, NL, FWR, CC, GS, LT, SC and MMC did the results interpretation. MO, NL did the initial manuscript drafting. MMC and SC made the first revision and, then, YA, AB, MC, LD, MDP, SH, DK, MK, GT, FL, VM, GM, AP made other revisions.

All Authors had full access to the database and the statistical analysis.

All Authors approved the final version of the manuscript.

Declaration of interests

- Stefano Colagrande reports personal fees from NOVARTIS-SANOFI-LILLY-CELTHER-PFIZER-JANSSEN, outside the submitted work;

- Masataka Kuwana reports grants and personal fees from Boehringer-Ingelheim, personal fees from Corbus, grants and personal fees from Chugai, grants and personal fees from Ono Pharmeceuticals, personal fees from Tanabe-Mitsubishi, personal fees from Astellas, personal fees from Gilead, personal fees from Mochida, outside the submitted work;

-Sara Tomassetti reports personal fees from Boehringer Ingelheim, personal fees from Roche, outside the submitted work;

- Gianluca Sambataro reports personal fees from Boehringer Ingelheim, outside the submitted work;

- Cosimo Bruni reports personal fees from Actelion, personal fees from Eli Lilly, grants from European Scleroderma Trial and Research (EUSTAR) group, grants from New Horizon Fellowship, grants from Foundation for Research in Rheumatology (FOREUM), grants from Fondazione Italiana per la Ricerca sull'Artrite (FIRA), outside the submitted work ;

- Carlo Vancheri reports grants and personal fees from Boehringer Ingelheim, grants and personal fees from F. Hoffmann-La Roche Ltd. , outside the submitted work;

- Fabrizio Luppi reports lectures fee from Roche and from Boehringer-Ingelheim;

- Christopher P. Denton reports grants and personal fees from GSK, personal fees from Boerhinger Ingelheim, grants from Servier, grants and personal fees from Inventiva, grants and personal fees from Arxx Therapeutics, personal fees from Corbus, personal fees from Sanofi, personal fees from Roche, outside the submitted work ;

- Federico Lavorini reports grants and personal fees from GSK, personal fees from Boehringer Ingelheim, personal fees from Orion Pharma, personal fees from AstraZeneca, grants from MSD, personal fees from HIKMA, personal fees from Trudell International, grants and personal fees from Chiesi Farmaceutici, personal fees from Novartis Pharma, outside the submitted work ;

- Michael Hughes reports personal fees from Speaking fees from Actelion, Eli lilly and Pfizer, outside the submitted work ;

- Dinesh Khanna reports personal fees from Actelion, grants and personal fees from Bayer, grants and personal fees from Boehringer Ingelhem, personal fees from CSL Behring, grants and personal fees from Horizon, grants from Pfizer, personal fees from Corbus, grants and personal fees from BMS, outside the submitted work; and Dr Khanna is the Chief Medical officer of Eicos Sciences Inc and has stock options, outside the submitted work
All other authors have declared no competing interests.

Financial support

No specific funding was received from any bodies in the public, commercial or not-for-profit sectors to carry out the work described in this article.

Data sharing

A deidentified dataset will be made available upon request to the corresponding author at least 1 year after the publication of this study. The request must include a statistical analysis plan.

TABLES

TABLE 1. READERS DIAGNOSTIC PERFORMANCE

	CORRECT DIAGNOSIS			RAD vs nRAD	Chest-RAD vs non -chest RAD
READERS	COVID-19	SSc-ILD	TOT (CI)		
nRAD	75.95% (499/657)	78.95% (510/646)	77.5% (75.13%-79.74%)	p=0.0008	
RAD	86.61% (304/351)	81.06% (270/333)	83.92% (80.95%-86.59%)		
Chest-RAD	88.40% (221/250)	84.58% (203/240)	86.53% (83.18%-89.43%)		p=0.0034
Non-Chest-RAD	82.18% (83/101)	72.04% (67/93)	77.32% (70.77%-83.01%)		

Legend

nRAD: non radiologist clinicians; RAD: radiologists; Chest-RAD: chest radiologists, with at least more than 5 years of experience in chest imaging, Non-Chest-RAD: radiologists without experience in chest imaging.

CI: Confidence Interval

CT PARAMETER	LEVEL	COVID-19	SSC-ILD	OR (95%CI)	p-VALUE	AUC (95%CI)	PREDICTIVE CAPABILITY	
FOCAL GGO with FIBROSIS UPPER ZONE	Absence	14(27.45%)	34(70.83%)	Reference	.			**Associated with SSc-ILD**
	No	37(72.55%)	6(12.5%)	0.07 (0.03 - 0.21)	<.0001*	0.82 (0.75 - 0.90)	Good	
	Yes	0(0%)	8(16.67%)	7.15 (0.33 - 156.76)	0.2120			
GGO with FIBROSIS LOWER ZONES	Absence	5(9.8%)	4(8.33%)	Reference	.			
	No	42(82.35%)	4(8.33%)	0.129 (0.025 - 0.667)	0.0145	0.908 (0.849 - 0.967)	Excellent	
	Yes	4(7.84%)	40(83.33%)	11 (2.131 - 56.794)	0.0042			
RETICULATIONS LOWER ZONE	No	49(96.08%)	7(14.58%)	Reference	.			
	Yes	2(3.92%)	41(85.42%)	109.59 (24.31 - 494.08)	<.0001*	0.91 (0.85 - 0.96)	Excellent	
RETICULATIONS SIDE LOWER ZONE	Absence	49(96.08%)	7(14.58%)	Reference	.			
	Bilateral, asymmetric	0(0%)	2(4.17%)	33.02 (0.74 - 1474.71)	0.0712	0.91 (0.85 - 0.96)	Excellent	
	Bilateral, symmetric	2(3.92%)	39(81.25%)	104.28 (23.08 - 471.10)	<.0001*			
RET with	Absence	49(96.08%)	7(14.58%)	Reference	.			

TABLE 2. DISCRIMINATING CT PARAMETERS.

FIBROSIS LOWER ZONE	No	1(1.96%)	2(4.17%)	11 (0.94 - 129.11)	0.0563	0.92 (0.86 - 0.97)	Excellent	
	Yes	1(1.96%)	39(81.25%)	173.8 (28.06 - 1076.39)	<.0001*			
CONSOLIDATION LOWER ZONE	No	8(15.69%)	44(91.67%)	Reference	.			**Associated with COVID-19 pneumonia**
	Yes	43(84.31%)	4(8.33%)	0.02 (0.00 - 0.07)	<.0001*	0.88 (0.82 - 0.94)	Good	
CONSOLIDATION SIDE LOWER ZONE	Absence	8(15.69%)	44(91.67%)	Reference	.			
	Unilateral	10(19.61%)	3(6.25%)	0.06 (0.01 - 0.27)	0.0002*	0.90 (0.84 - 0.96)	Excellent	
	Bilateral, asymmetric	16(31.37%)	0(0%)	0.01 (0 - 0.11)	0.0007*			
	Bilateral, symmetric	17(33.33%)	1(2.08%)	0.02(0.00 - 0.11)	<.0001*			
CONSOLIDATION C/P DISTRIBUTION LOWER ZONE	Absence	8(15.69%)	44(91.67%)	Reference	.			
	Central	1(1.96%)	0(0%)	0.06 (0.00 - 6.24)	0.2402	0.89 (0.82 - 0.95)	Good	
	Peripherical	32(62.75%)	3(6.25%)	0.02 (0.00 - 0.08)	<.0001*			
	No prevalence	5(9.8%)	0(0%)	0.02 (0.00 - 0.45)	0.0147*			
	Patchy	5(9.8%)	1(2.08%)	0.05 (0.01 - 0.42)	0.0055*			
CONSOLIDATION A/P	Absence	8(15.69%)	44(91.67%)	Reference	.			
	mostly anterior	4(7.84%)	0(0%)	0.02 (0.00 - 0.60)	0.0242*	0.88 (0.82 -	Good	

DISTRIBUTION LOWER ZONE						0.95)		
	mostly posterior	33(64.71%)	3(6.25%)	0.02 (0.00 - 0.08)	<.0001*			
	no predominance	6(11.76%)	1(2.08%)	0.04 (0.01 - 0.34)	0.0027*			
GGO ROUNDED LOWER ZONE	Absence	5(9.8%)	4(8.33%)	3.32 (0.74 - 14.81)	0.1165	0.81 (0.73 - 0.89)	Good	
	Rounded	38(74.51%)	9(18.75%)	Reference	.			
	Non rounded	8(15.69%)	35(72.92%)	16.93 (5.96 - 48.04)	<.0001*			

Legend:
Detailed results of all CT parameters analysed.
*P<0.05
SSC-ILD: interstitial lung disease secondary to Systemic sclerosis ; OR : Odds Ratio ; CI :Confidence Interval; AUC: Area under Curve; C/P: Central /Peripheral; A/P: Anterior/Posterior; GGO: Ground glass opacities; Absence: absence of the alteration for which the sub analysis should have been performed.

TABLE 3. MULTIVARIATE ANALYSIS WITH BACKWARD SELECTION METHOD RESULTS

CT PARAMETER	LEVEL	OR (95%CI)	p-VALUE	AUC (95%CI)
CONSOLIDATION LOWER ZONE	No	reference		0.97 (0.94-1.00 CI)
	Yes	69.41 (7.81-616.801)	0.0001*	
GGO with FIBROSIS LOWER ZONE	Absence	21.65 (1.51-310.0)	0.0236*	
	No	119 .61 (12.13-999.99)	<0.0001 *	
	Yes	reference		
FOCAL GGO with FIBROSIS UPPER ZONE		excluded	0.99	
RETICULATIONS LOWER ZONE		excluded	0.89	
ROUNDED GGO LOWER ZONE		excluded	0.97	

Legend
GGO: Ground glass opacities; Absence: Absence of the alterations for which the sub analysis should have been performed.
OR : Odds Ratio ; CI: Confidence Interval; AUC: Area under Curve
*P<0.05

FIGURES

FIGURE 1. THE CLINICAL INTERPRETATION OF THE COVID-19 PNEUMONIA PREDICTIVE SCORE.

Legend:
A-C: High probability for COVID-19 pneumonia; D: Probably COVID-19 pneumonia in SSc-ILD; E-F: Low probability for COVID-19 pneumonia.
Ssc: systemic sclerosis; ILD: interstitial lung disease; GGO: ground glass opacities; RET: reticulations, HC: honeycombing.

FIGURE 2. COVID-19 PNEUMONIA IN PATIENT WITH SSc-ILD

Legend
Covid pneumonia in SSc patients. Basal smooth RET (white arrow), in presence of pleural effusion, and GGO (black arrows), were considered as manifestation of disease other than Covid pneumonia and/or SSc-ILD (pulmonary edema), by most of readers.
Ssc: systemic sclerosis; ILD: interstitial lung disease; GGO: ground glass opacities; RET: reticulations.

FIGURE 3. FOCAL FIBROSIS INSIDE GGO, GGO WITH AND WITHOUT FIBROSIS

Legend
A: Ssc-ILD, right lung, upper zone. Focal alteration with bronchiectasis at the periphery of upper lobe, configuring signs of fibrosis (white arrow).
B: SSc-ILD, lower zone. Bilateral diffuse GGO with bronchiectasis, configuring signs of fibrosis (white arrow)

C: COVID-19, lower right lobe: GGO without fibrosis (white arrow).
SSc: systemic sclerosis; ILD: interstitial lung disease; GGO: ground glass opacities.

REFERENCES

1 CDC COVID-19 Response Team. Preliminary estimates of the prevalence of selected underlying health conditions among patients with coronavirus disease 2019 - United States, February 12-March 28, 2020. *MMWR Morb Mortal Wkly Rep* 2020; 69: 382-6

2 Orlandi M, Lepri G, Damiani A, Barsotti S, Di Battista M, Codullo V,et al. One year in review 2020: systemic sclerosis. *Clin Exp Rheumatol.* 2020;38 Suppl 125(3):3-17.

3 Volkmann ER. Natural history of systemic sclerosis–related interstitial lung disease: How to identify a progressive fibrosing phenotype. *J Scleroderma Relet Disord* 2020; 5(2S): 31-40.

4 Fujita J, Yoshinouchi T, Ohtsuki Y, Tokuda M, Yang Y, Yamadori I, et al. Non-specific interstitial pneumonia as pulmonary involvement of systemic sclerosis. *Ann Rheum Dis.* 2001;60(3):281-3.

5 Orlandi M, Lepri G, Bruni C, Wang Y, Bartoloni A, Zammarchi L, et al. The systemic sclerosis patient in the COVID-19 era: the challenging crossroad between immunosuppression, differential diagnosis and long-term psychological distress. *Clin Rheumatol.* 2020;39(7):2043-2047.

6 Orlandi M, Landini N, Bruni C, Colagrande S, Matucci-Cerinic M, Kuwana M. Infection or Autoimmunity? The Clinical Challenge of Interstitial Lung Disease in Systemic Sclerosis During the COVID-19 Pandemic. *J Rheumatol*. 2020 Dec 1:jrheum.200832.

7 Landini N, Orlandi M, Fusaro M, Ciet P, Nardi C, Bertolo S, et al. The Role of Imaging in COVID-19 Pneumonia Diagnosis and Management: Main Positions of the Experts, Key Imaging Features and Open Answers. *J Cardiovasc Echogr.* 2020;30(Suppl 2):S25-S30.

8 Goldin JG, Lynch DA, Strollo DC, Suh RD, Schraufnagel DE, Clements PJ, et al. High-resolution CT scan findings in patients with symptomatic scleroderma-related interstitial lung disease. *Chest.* 2008;134(2):358-367.

9 Volkmann ER. Natural history of systemic sclerosis–related interstitial lung disease: How to identify a progressive fibrosing phenotype. *Journal of Scleroderma and Related Disorders*. 2020;5(2_suppl):31-40.

10 Launay D, Remy-Jardin M, Michon-Pasturel U, Mastora I, Hachulla E, Lambert M,et al. High resolution computed tomography in fibrosing alveolitis associated with systemic sclerosis. *J Rheumatol*. 2006;33(9):1789-801. PMID: 16960939.

11 Desai SR, Veeraraghavan S, Hansell DM, Nikolakopolou A, Goh NS, Nicholson AG, et al. CT features of lung disease in patients with systemic sclerosis: comparison with idiopathic pulmonary fibrosis and nonspecific interstitial pneumonia. *Radiology*. 2004;232(2):560-7.

12 King TE Jr. Nonspecific interstitial pneumonia and systemic sclerosis. *Am J Respir Crit Care Med*. 2002; 165:1578–9.

13 Rubin GD, Ryerson CJ, Haramati LB, Sverzellati N, Kanne JP, Raoof S, et al. The Role of Chest Imaging in Patient Management during the COVID-19 Pandemic: A Multinational Consensus Statement from the Fleischner Society. *Radiology.* 2020 Jul;296(1):172-180.

14 Simpson S, Kay FU, Abbara S, Bhalla S, Chung JH, Chung M, et al. Radiological Society of North America Expert Consensus Statement on Reporting Chest CT Findings Related to COVID-19. Endorsed by the Society of Thoracic Radiology, the American College of Radiology, and RSNA - Secondary Publication. *J Thorac Imaging*. 2020;35(4):219-227.

15 van den Hoogen F, Khanna D, Fransen J, Johnson SR, Baron M, Tyndall A, et al. 2013 classification criteria for systemic sclerosis: an American College of Rheumatology/European League against Rheumatism collaborative initiative. *Arthritis Rheum*. 2013;65(11):2737-47.

16 Prosch H, Schaefer-Prokop CM, Eisenhuber E, Kienzl D, Herold CJ. CT protocols in interstitial lung diseases--a survey among members of the European Society of Thoracic Imaging and a review of the literature. Eur Radiol. 2013 Jun;23(6):1553-63.

17 Nishino M, Itoh H, Hatabu H. A practical approach to high-resolution CT of diffuse lung disease. *Eur J Radiol*. 2014;83(1):6-19.

18 Hansell DM, Bankier AA, MacMahon H, McLoud TC, Müller NL, Remy J. Fleischner Society: glossary of terms for thoracic imaging. *Radiology*. 2008;246(3):697-722.

19 Bai HX, Hsieh B, Xiong Z, Halsey K, Choi JW, Tran TML, et al. Performance of Radiologists in Differentiating COVID-19 from Non-COVID-19 Viral Pneumonia at Chest CT. *Radiology.* 2020;296(2):E46-E54.

20 Calabrò L, Peters S, Soria JC, Di Giacomo AM, Barlesi F, Covre A, et al. Challenges in lung cancer therapy during the COVID-19 pandemic. *Lancet Respir Med.* 2020;8(6):542-544.

21 Rodriguez-Morales AJ, Cardona-Ospina JA, Gutiérrez-Ocampo E, Villamizar-Peña R, Holguin-Rivera Y, Escalera-Antezana JP, et al. Clinical, laboratory and imaging features of COVID-19: A systematic review and meta-analysis. *Travel Med Infect Dis*. 2020;34:101623.

22 Yang J, Zheng Y, Gou X, Pu K, Chen Z, Guo Q, et al. Prevalence of comorbidities and its effects in patients infected with SARS-CoV-2: a systematic review and meta-analysis. *Int J Infect Dis*. 2020;94:91-95.

23 Chen N, Zhou M, Dong X, Qu J, Gong F, Han Y, et al. Epidemiological and clinical characteristics of 99 cases of 2019 novel coronavirus pneumonia in Wuhan, China: a descriptive study. *Lancet.* 2020;395(10223):507-513.

24 Capobianco J, Grimberg A, Thompson BM, Antunes VB, Jasinowodolinski D, Meirelles GS. Thoracic manifestations of collagen vascular diseases. *Radiographics*. 2012;32(1):33-50.

25 Cheng C, Li C, Zhao T, Yue J, Yang F, Yan Y, et al. COVID-19 with rheumatic diseases: a report of 5 cases. *Clin Rheumatol*. 2020;39(7):2025-2029.

26 Mariano RZ, Rio APTD, Reis F. Covid-19 overlapping with systemic sclerosis. *Rev Soc Bras Med Trop*. 2020 Sep 21;53:e20200450.

CT IMAGES	LEGEND	TOTAL CT SCORE	P	CT IMAGES	LEGEND	TOTAL CT SCORE	P
A 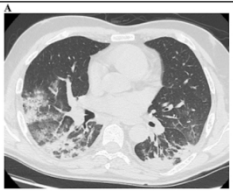	Presence of CONS in lower zone (4 points) Presence of GGO without fibrosis in lower zone (5 points)	4+5= 9	5-9 points: HIGH PROBABILITY for COVID -19 PNEUMONIA	D 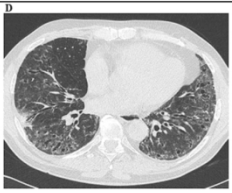	Presence of CONS (4 points) in lower zone Presence of GGO with fibrosis in lower zone	4	4 points: PROBABLY COVID-19 PNEUMONIA in SSC-ILD
B 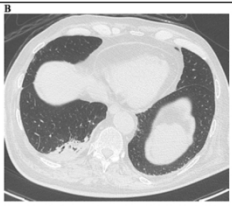	Presence of CONS in lower zone (4 points) Absence of GGO in lower zone (3 points)	4+3= 7		E 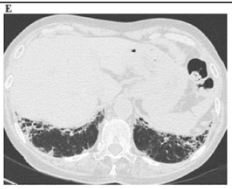	Absence of GGO (3 points) in lower zone, presence of HC and RET.	3	0-3 points:
C 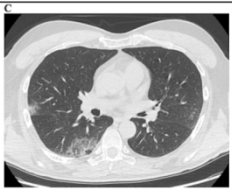	Presence of GGO without fibrosis in lower zone (5 points) Absence of CONS in lower zone	5		F 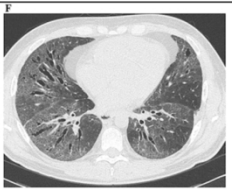	Absence CONS in lower zone (0 point), GGO with fibrosis in lower zone (0 point)	0	LOW PROBABILITY for COVID-19 PNEUMONIA

160x106mm (300 x 300 DPI)

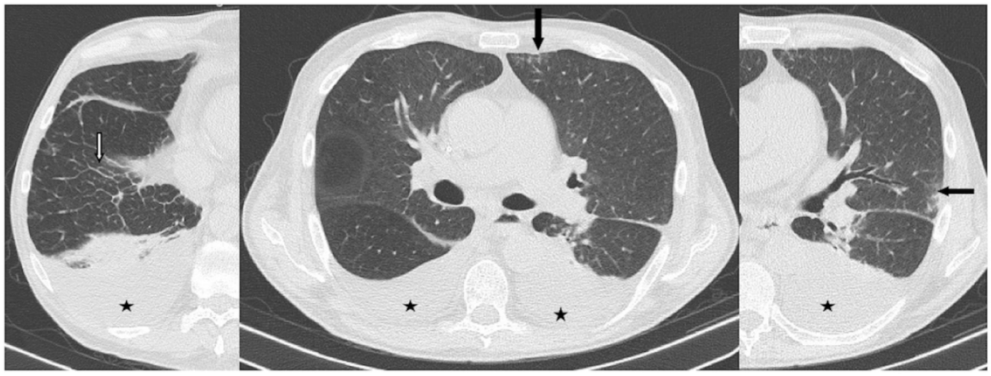

159x61mm (300 x 300 DPI)

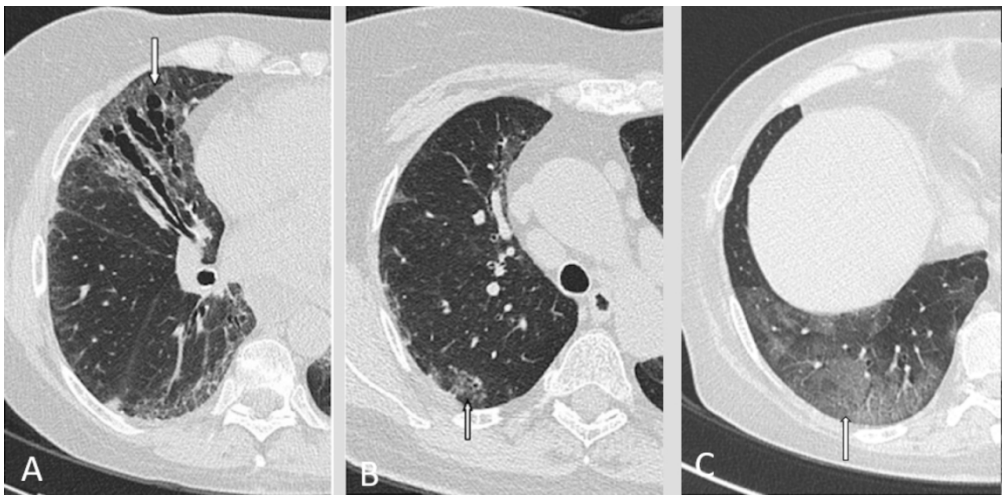

119x58mm (300 x 300 DPI)

Supplementary Figure S1.

CT COVID-19 PATTERN: MULTIFOCAL AND DIFFUSE PATTERN

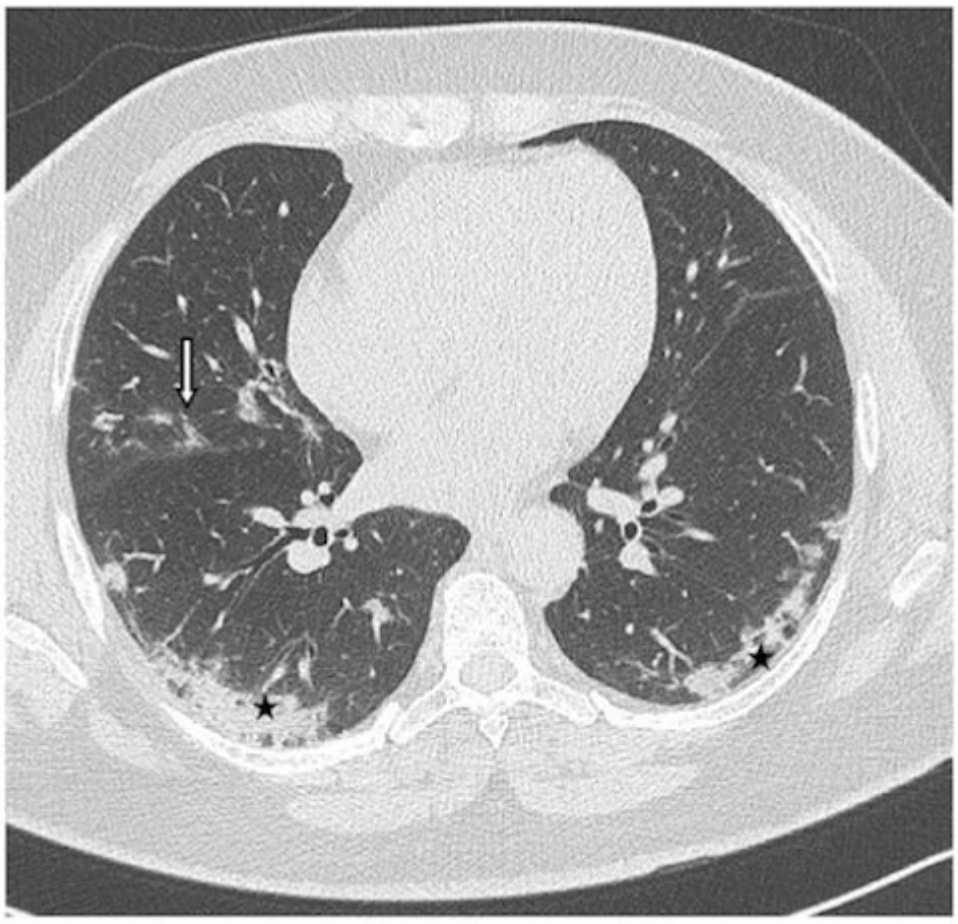

Legend

Covid 19 pneumonia presenting with multifocal and diffuse pattern. Peripheral alterations with irregural shape and a maximum diameter > 3cm configure a diffuse pattern (black stars). Focal alterations are also present (white arrow).

Supplementary Figure S2.

SCORE PREDICTIVE CAPABILITY IN COVID-19 DIAGNOSIS

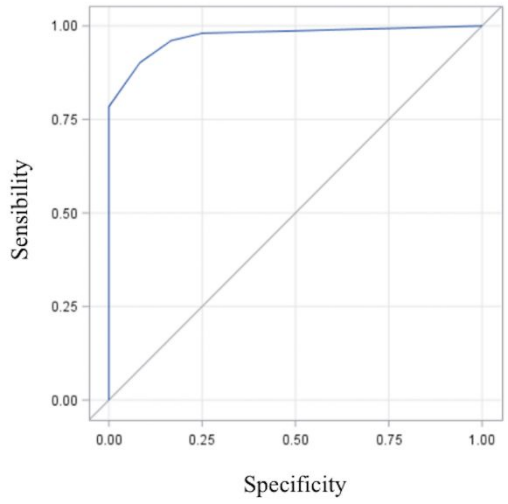

Legend

The probability of making a correct COVID -19 pneumonia diagnosis increases with the increment of the score. The score identified has an excellent predictive ability: the area under the ROC curve is 0.97 (0.97-1.00 CI).

Supplementary Figure S3.

RAD INTER-READER LOW AGREEMENT FOR HC AND RET DETECTION IN UPPER ZONE

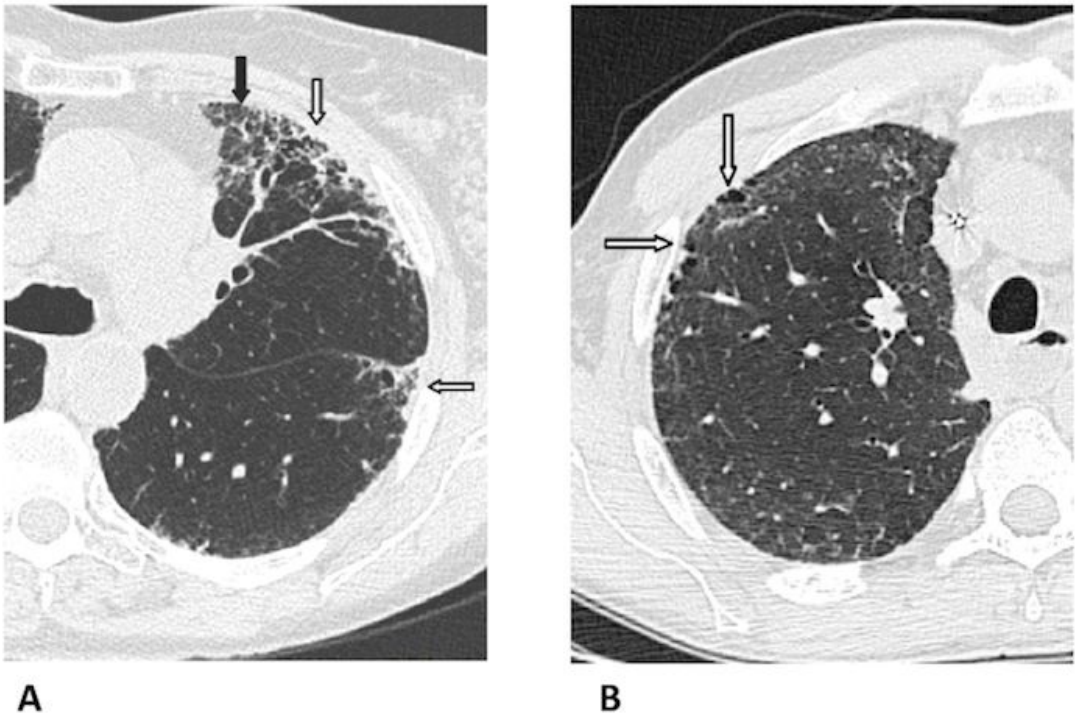

Legend

A: SSc-ILD, right lung, upper zone. Chest RAD may interpret peripheral alterations in the right upper lobe (white arrow) as HC or paraseptal emphysema.

B: SSc-ILD, left lung, upper zone. Peripheral RET (white arrows). Some lesion may be differently considered as GGO or tiny RET by chest RAD readers (black arrow).

SSc: systemic sclerosis; ILD: interstitial lung disease; RET: Reticulations; HC: honeycombing; GGO: ground glass opacities; RAD: radiologist group.

Supplementary Figure S4.

CONSOLIDATION IN LOWER ZONES

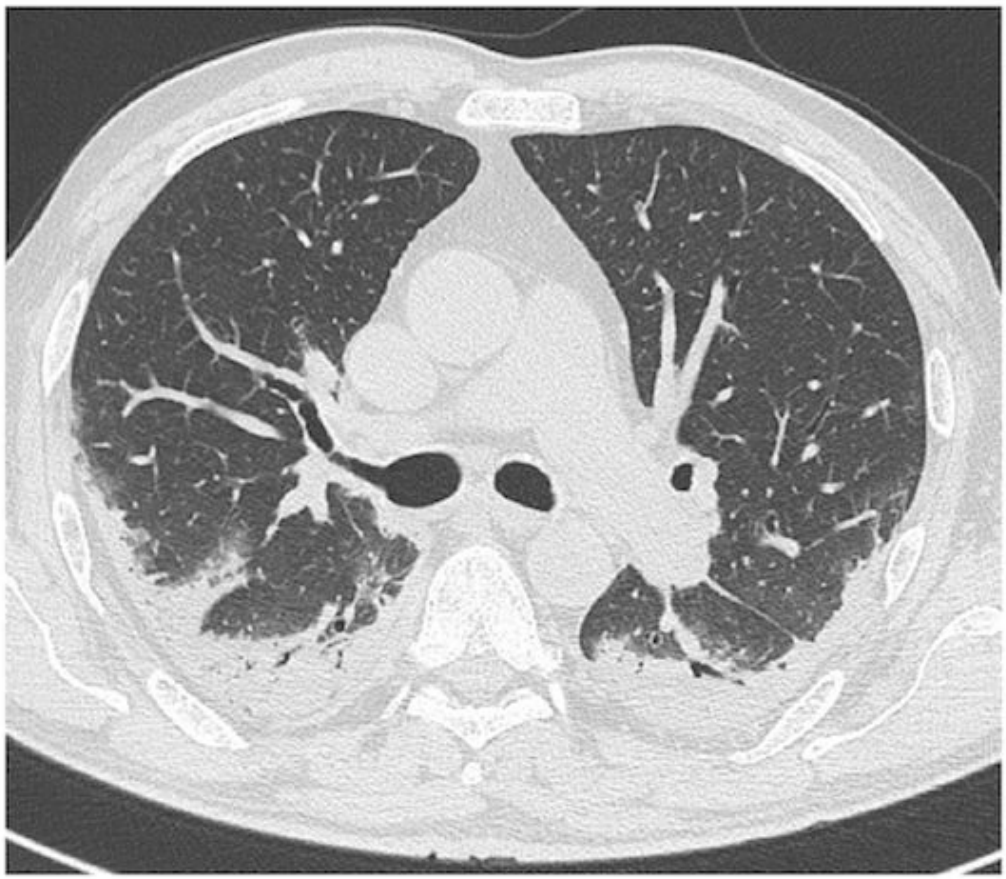

Legend

Covid 19 pneumonia, lower zone. Bilateral, symmetric, peripheral consolidations.

Supplementary Figure S5.

ROUNDED GGO

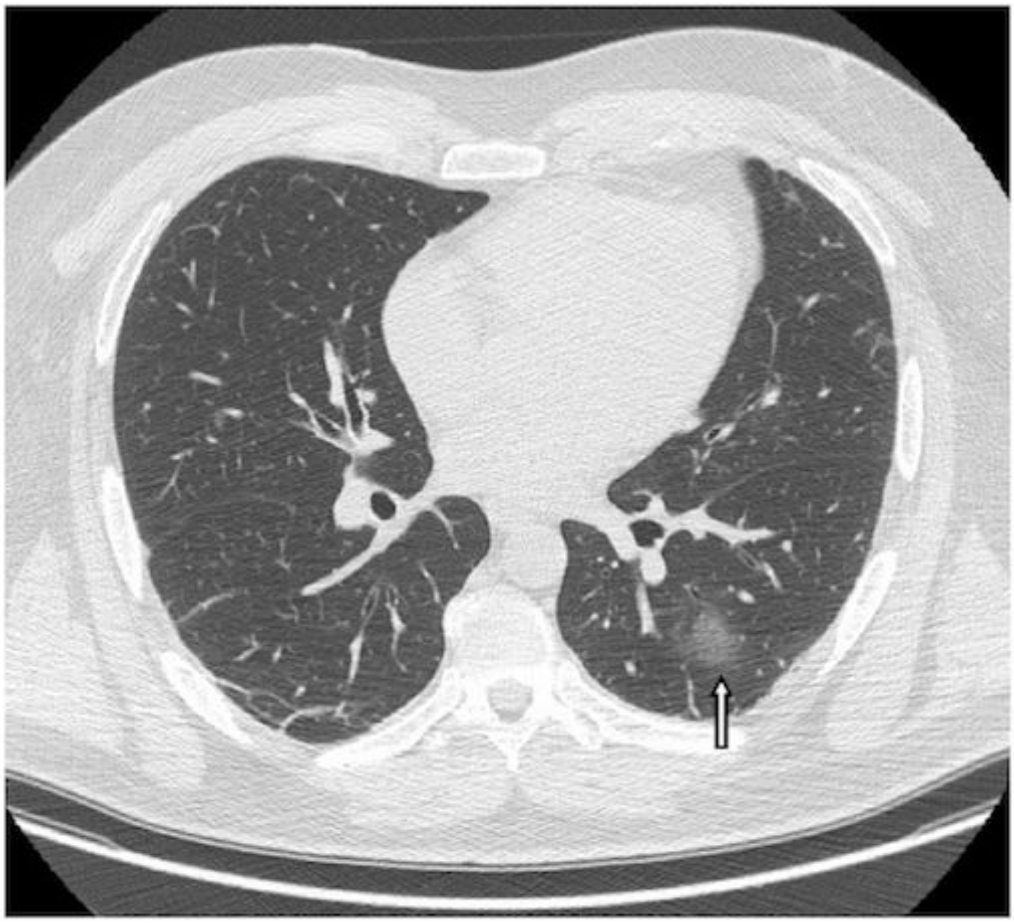

Legend

Covid 19 pneumonia. Rounded focal GGO in the left lower lobe, lower zone (white arrow).

GGO: ground glass opacities

Supplementary Table S1. Inter-reader agreement

CT PARAMETER	nRAD COHEN'S K (LCL95%-UCL95%)	RAD COHEN'S K (LCL95%-UCL95%)	nRAD VS RAD p-VALUE	Chest RAD COHEN'S K (LCL95%-UCL95%)	n-chest-RAD COHEN'S K (LCL95%-UCL95%)	n-chest-RAD VS chest-RAD p-VALUE
WHOLE LUNG PARENCHYMA						
Pattern	-	0.48(0.41-0.56)*	.	0.48(0.41-0.56)*	-	.
Upper/Lower	0.19(0.18-0.2)	0.31(0.27-0.34)	<.0001	0.41(0.36-0.47)*	0.14(0-0.29)	0.0006
Bilateral/Simmetrical	0.26(0.25-0.28)	0.46(0.42-0.49)*	<.0001	0.51(0.46-0.57)*	0.38(0.24-0.53)	0.0984
Right lung involvement	0.15(0.14-0.16)	0.60(0.58-0.63)**	<.0001	0.63(0.6-0.67)**	0.64(0.53-0.75)**	0.9221
Left lung involvement	0.19(0.18-0.21)	0.50(0.47-0.53)*	<.0001	0.57(0.52-0.62)*	0.47(0.34-0.6)*	0.1632
Central vs Peripheral	0.16(0.14-0.17)	0.27(0.24-0.29)	<.0001	0.43(0.39-0.47)*	0.15(0.02-0.28)	<.0001
Anterior vs Posterior	0.18(0.17-0.19)	0.28(0.24-0.31)	<.0001	0.34(0.29-0.4)	0.27(0.11-0.42)	0.3576
UPPER ZONE						
CONSOLIDATION						
Presence	0.25(0.24-0.27)	0.60(0.56-0.64)*	<.0001	0.66(0.6-0.72)**	0.39(0.2-0.58)	0.0081
Bilateral/Simmetrical	0.09(0.08-0.11)	0.48(0.45-0.5)*	<.0001	0.57(0.53-0.61)*	0.27(0.14-0.4)	<.0001
Central/Peripheral	0.11(0.1-0.12)	0.49(0.46-0.52) *	<.0001	0.57(0.52-0.61)*	0.31(0.15-0.47)	0.0023
Anterior/Posterior	0.11(0.1-0.12)	0.52(0.49-0.55) *	<.0001	0.60(0.56-0.64)*	0.32(0.16-0.47)	0.0004
Air bronchogram	0.08(0.07-0.09)	0.43(0.4-0.46) *	<.0001	0.51(0.46-0.55)*	0.24(0.11-0.37)	0.0002
Organising pneumonia	-	0.27(0.24-0.3)	.	0.51(0.46-0.55)*	0.59(0.43-0.74)*	0.3160
Fibrosis	-	0.35(0.32-0.39)	.	0.63(0.58-0.68)**	0.35(0.21-0.48)	0.0001
GGO						
Presence	0.21(0.19-0.22)	0.48(0.44-0.52) *	<.0001	0.54(0.48-0.6)*	0.36(0.18-0.54)	0.0619
Pattern	-	0.39(0.32-0.45)	.	0.39(0.32-0.45)	-	.
Bilateral/Simmetrical	0.15(0.14-0.16)	0.45(0.42-0.47) *	<.0001	0.52(0.48-0.56)*	0.32(0.2-0.44)	0.0018

CT PARAMETER	nRAD COHEN'S K (LCL95%-UCL95%)	RAD COHEN'S K (LCL95%-UCL95%)	nRAD VS RAD p-VALUE	Chest RAD COHEN'S K (LCL95%-UCL95%)	n-chest-RAD COHEN'S K (LCL95%-UCL95%)	n-chest-RAD VS chest-RAD p-VALUE
Central/Peripheral	0.12(0.11-0.13)	0.34(0.31-0.36)	<.0001	0.47(0.43-0.5)*	0.21(0.08-0.34)	0.0001
Anterior/Posterior	0.14(0.13-0.15)	0.41(0.38-0.43) *	<.0001	0.48(0.44-0.52)*	0.33(0.21-0.45)	0.0275
Rounded/Non rounded	-	0.48(0.4-0.57) *	.	0.48(0.4-0.57)*		.
Fibrosis	-	0.41(0.38-0.44) *	.	0.54(0.49-0.58)*	0.23(0.08-0.38)	<.0001
Fibrosis in focal lesions	-	0.63(0.53-0.73) **	.	0.63(0.53-0.73)**		
CRAZY PAVING						
Presence	0.14(0.13-0.15)	0.36(0.32-0.4)	<.0001	0.47(0.41-0.53)*	0.3(0.12-0.48)	0.0885
Bilateral/Simmetrical	0.04(0.03-0.05)	0.27(0.24-0.3)	<.0001	0.35(0.3-0.39)	0.25(0.12-0.39)	0.2001
Central/Peripheral	0.03(0.01-0.04)	0.31(0.28-0.34)	<.0001	0.44(0.4-0.48)*	0.20(0.06-0.34)	0.0014
Anterior/posterior	0.03(0.02-0.04)	0.31(0.28-0.34)	<.0001	0.40(0.36-0.45)*	0.25(0.1-0.4)	0.0554
RETICULATIONS						
Presence	0.18(0.17-0.2)	0.45(0.41-0.49)*	<.0001	0.38(0.32-0.44)	0.57(0.37-0.76)*	0.0717
Bilateral/Simmetrical	0.11(0.1-0.12)	0.55(0.51-0.58)*	<.0001	0.56(0.51-0.61)*	0.51(0.36-0.66)*	0.5490
Central/Peripheral	0.12(0.11-0.13)	0.60(0.56-0.64)**	<.0001	0.61(0.55-0.66)**	0.59(0.41-0.78)*	0.8741
Anterior/Posterior	0.09(0.08-0.1)	0.51(0.48-0.54)*	<.0001	0.55(0.51-0.6)*	0.39(0.26-0.52)	0.0201
Fibrosis	-	0.46(0.43-0.49)*	.	0.65(0.6-0.7)**	0.45(0.31-0.58)*	0.0065
HONEY COMBING						
Presence	0.16(0.15-0.18)	0.39(0.35-0.43)	<.0001	0.39(0.33-0.45)	0.37(0.18-0.56)	0.8314
Bilateral/Simmetrical	0.07(0.05-0.08)	0.35(0.31-0.38)	<.0001	0.34(0.29-0.38)	0.34(0.2-0.49)	0.9309
Central/Peripheral	0.05(0.03-0.06)	0.36(0.32-0.39)	<.0001	0.36(0.31-0.42)	0.35(0.17-0.53)	0.8514
Anterior/posterior	0.03(0.01-0.04)	0.31(0.28-0.34)	<.0001	0.36(0.32-0.41)	0.26(0.11-0.4)	0.1693
VESSEL TICKENING	-	0.09(0.05-0.13)	.	0.27(0.21-0.33)	0.46(0.27-0.64)*	0.0677
SUBPLEURAL LINES	-	0.28(0.23-0.32)	.	0.34(0.28-0.4)	0.09(0-0.26)	0.0078

CT PARAMETER	nRAD COHEN'S K (LCL95%-UCL95%)	RAD COHEN'S K (LCL95%-UCL95%)	nRAD VS RAD p-VALUE	Chest RAD COHEN'S K (LCL95%-UCL95%)	n-chest-RAD COHEN'S K (LCL95%-UCL95%)	n-chest-RAD VS chest-RAD p-VALUE
LOWER ZONE						
CONSOLIDATION						
Presence	0.28(0.27-0.3)	0.62(0.58-0.66)**	<.0001	0.71(0.65-0.77)**	0.46(0.27-0.64)*	0.0124
Bilateral/Simmetrical	0.14(0.13-0.15)	0.52(0.49-0.54)*	<.0001	0.59(0.55-0.63)*	0.38(0.25-0.5)	0.0017
Central/Peripheral	0.15(0.14-0.16)	0.55(0.52-0.59)*	<.0001	0.62(0.57-0.67)**	0.46(0.28-0.63)*	0.0755
Anterior/Posterior	0.17(0.16-0.18)	0.56(0.52-0.59)*	<.0001	0.62(0.57-0.67)**	0.47(0.31-0.63)*	0.0968
Air bronchogram	0.14(0.13-0.15)	0.43(0.4-0.46)*	<.0001	0.51(0.47-0.55)*	0.26(0.12-0.4)	0.0005
Organising pneumonia	-	0.31(0.28-0.34)	.	0.52(0.47-0.56)*	0.36(0.21-0.5)	0.0352
Fibrosis	-	0.20(0.17-0.23)	.	0.27(0.22-0.31)	0.31(0.17-0.44)	0.5832
GROUND GLASS OPACITY						
Presence	0.15(0.14-0.17)	0.31(0.27-0.35)	<.0001	0.45(0.39-0.51)*	0.16(0-0.35)	0.0036
	-	0.47(0.4-0.55)*	.	0.47(0.4-0.55)*	-	.
Pattern	-	0.47(0.4-0.55)	-	0.47(0.4-0.55)	-	
Bilateral/Simmetrical	0.12(0.11-0.14)	0.41(0.38-0.44)*	<.0001	0.52(0.48-0.57)*	0.17(0.05-0.3)	<.0001
Central/Peripheral	0.10(0.09-0.11)	0.22(0.19-0.24)	<.0001	0.34(0.3-0.37)	0.11(0-0.24)	0.0012
Anterior/Posterior	0.09(0.08-0.1)	0.30(0.27-0.33)	<.0001	0.37(0.33-0.42)	0.18(0.05-0.31)	0.0063
Rounded/Not rounded	-	0.62(0.53-0.72) **	.	0.62(0.53-0.72)**		.
Fibrosis	-	0.46(0.42-0.49) *	.	0.64(0.59-0.69)**	0.09(0-0.26)	<.0001
Fibrosis in focal lesions	-	0.56(0.46-0.65) *	.	0.56(0.46-0.65)*		.
CRAZY PAVING						
Presence	0.11(0.1-0.13)	0.26(0.22-0.3)	<.0001	0.39(0.33-0.45)	0.07(0-0.25)	0.0010
Bilateral/Simmetrical	0.05(0.04-0.06)	0.21(0.18-0.24)	<.0001	0.30(0.26-0.35)	0.11(0-0.26)	0.0120

CT PARAMETER	nRAD COHEN'S K (LCL95%-UCL95%)	RAD COHEN'S K (LCL95%-UCL95%)	nRAD VS RAD p-VALUE	Chest RAD COHEN'S K (LCL95%-UCL95%)	n-chest-RAD COHEN'S K (LCL95%-UCL95%)	n-chest-RAD VS chest-RAD p-VALUE
Central/Peripheral	0.03(0.02-0.04)	0.24(0.21-0.27)	<.0001	0.36(0.32-0.4)	0.05(0-0.2)	0.0001
Anterior/posterior	0.03(0.02-0.04)	0.23(0.2-0.26)	<.0001	0.35(0.3-0.39)	0.06(0-0.2)	0.0001
RETICULATIONS						
Presence	0.25(0.23-0.26)	0.71(0.67-0.75) **	<.0001	0.75(0.69-0.81)**	0.58(0.39-0.76)*	0.0714
Bilateral/Simmetrical	0.16(0.15-0.17)	0.66(0.62-0.69)**	<.0001	0.70(0.65-0.76)**	0.52(0.37-0.67)*	0.0208
Central/Peripheral	0.14(0.13-0.15)	0.51(0.48-0.54)*	<.0001	0.54(0.5-0.58)*	0.53(0.36-0.7)*	0.8719
Anterior/posterior	0.13(0.12-0.14)	0.51(0.48-0.54)*	<.0001	0.55(0.51-0.6)*	0.39(0.25-0.53)	0.0288
Fibrosis	-	0.51(0.48-0.54)*	.	0.74(0.69-0.8)**	0.39(0.25-0.53)	<.0001
HONEY COMBING						
Presence	0.36(0.34-0.37)	0.52(0.48-0.56)*	<.0001	0.57(0.51-0.63)*	0.46(0.27-0.64)*	0.2403
Bilateral/Simmetrical	0.21(0.2-0.22)	0.44(0.41-0.47)*	<.0001	0.46(0.41-0.51)*	0.41(0.26-0.56)*	0.5279
Central/Peripheral	0.19(0.18-0.21)	0.45(0.41-0.48)*	<.0001	0.47(0.42-0.52)*	0.40(0.22-0.58)	0.4397
Anterior/Posterior	0.18(0.17-0.19)	0.38(0.35-0.41)	<.0001	0.41(0.37-0.46)*	0.28(0.14-0.42)	0.0769
VESSEL TICKENING	-	0.06(0.02-0.11)	.	0.24(0.18-0.3)	0.55(0.36-0.74)*	0.0023
SUBPLEURAL LINES	-	0.26(0.22-0.31)	.	0.41(0.34-0.47)*	0.09(0-0.28)	0.0018
PLEURAL AND MEDIASTINAL INVOLVMENT						
Pleural thickening	0.04(0.03-0.06)	0.12(0.08-0.16)	0.0007	0.21(0.14-0.27)	0.33(0.14-0.52)	0.2165
Pleural retraction	-	0.20(0.16-0.24)	.	0.44(0.38-0.5)*	0.12(0-0.31)	0.0013
Pleural effusion	0.19(0.18-0.2)	0.56(0.53-0.59)*	<.0001	0.65(0.6-0.7)**	0.44(0.3-0.58)*	0.0060
Pericardial effusion	0.06(0.05-0.07)	0.25(0.21-0.29)	<.0001	0.26(0.2-0.32)	0.23(0.06-0.41)	0.7935
Dilated oesophagus	0.27(0.25-0.28)	0.60(0.56-0.64)**	<.0001	0.59(0.53-0.65)*	0.55(0.36-0.74)*	0.6974
Lymphoadenopathy	0.04(0.03-0.06)	0.34(0.3-0.39)	<.0001	0.40(0.34-0.46)	0.04(0-0.23)	0.0003
SCORES						

CT PARAMETER	nRAD COHEN'S K (LCL95%-UCL95%)	RAD COHEN'S K (LCL95%-UCL95%)	nRAD VS RAD p-VALUE	Chest RAD COHEN'S K (LCL95%-UCL95%)	n-chest-RAD COHEN'S K (LCL95%-UCL95%)	n-chest-RAD VS chest-RAD p-VALUE
COVID-19 (RSNA)	-	0.33(0.3-0.36)	.	0.41(0.37-0.45)*	0.31(0.18-0.43)	0.1293
CO-RADS	-	0.30(0.28-0.32)	.	0.36(0.33-0.4)	0.26(0.16-0.37)	0.0729

Legend: Total detailed results of inter-reader agreement.

*Discrete inter-readers agreement; ** Good inter-readers agreement

nRAD: non radiologist clinicians; RAD: radiologists; Chest-RAD: chest radiologists, with at least more than 5 years of experience; n-chest-RAD: radiologists without chest experience.

CT PARAMETER	VARIABLE	COVID-19	SSC-ILD	OR (95%CL)	p-VALUE		AURC (95%CL)	PREDICTIVE CAPABILITY
WHOLE LUNG PARENCHYMA								
PATTERN	Monofocal	2(3.92%)	0(0%)	0.36 (0.01 - 15.48)	0.5929		0.82 (0.75 - 0.89)	Good
	Multifocal	13(25.49%)	0(0%)	0.07 (0 - 1.32)	0.0753			
	Diffuse	7(13.73%)	29(60.42%)	7.03 (2.55 - 19.42)	0.0002*			
	(Multi)focal and diffuse	29(56.86%)	16(33.33%)		.			
	White lung	0(0%)	3(6.25%)	12.52 (0.39 - 404.37)	0.1541			
SIDE	Unilateral	5(9.8%)	1(2.08%)	0.19 (0.03 - 1.4)	0.1021		0.66 (0.57 - 0.74)	Scarse
	Bilateral, asymmetric	18(35.29%)	6(12.5%)	0.24 (0.09 - 0.68)	0.0069*			
	Bilateral, symmetric	28(54.9%)	41(85.42%)		.			
RIGHT LOBES INVOLVEMENT	No involvement	1(1.96%)	1(2.08%)	0.79 (0.05 - 13.15)	0.8715			
	Upper and lower	6(11.76%)	0(0%)	0.06 (0 - 1.41)	0.0808			
	Lower	4(7.84%)	2(4.17%)	0.44 (0.08 - 2.48)	0.3530			
	Medium	1(1.96%)	0(0%)	0.24 (0 - 25.35)	0.5507			
	Medium and upper	2(3.92%)	0(0%)	0.16 (0 - 6.72)	0.3353			
	Medium and lower lobes	2(3.92%)	2(4.17%)	0.79 (0.11 - 5.92)	0.8715			
	All lobes	34(66.67%)	43(89.58%)		.			
LEFT LOBES INVOLVEMENT	No involvement	1(1.96%)	0(0%)	0.28 (0 - 29.13)	0.5913			
	Upper	2(3.92%)	0(0%)	0.18 (0 - 7.71)	0.3734			
	Lower	6(11.76%)	2(4.17%)	0.35 (0.07 - 1.75)	0.2011			
	Both	42(82.35%)	46(95.83%)		.			
LOCALIZATION	Upper	6(11.76%)	0(0%)	0.05 (0 - 1.16)	0.0615		0.67 (0.58 - 0.76)	Scarse

Supplementary Table S2. CT parameters predictive capability

	Lower	25(49.02%)	39(81.25%)		.			
	No predominance	20(39.22%)	9(18.75%)	0.3 (0.12 - 0.76)	0.0109*			
ANTERIOR/POSTERIOR DISTRIBUTION	Anterior	3(5.88%)	1(2.08%)	0.73 (0.08 - 6.63)	0.7825		0.67 (0.58 - 0.76)	Scarse
	Posterior	38(74.51%)	22(45.83%)		.			
	No predominance	9 (17.65%)	24(50%)	4.41 (1.75-11.11)	0.0016			
CENTRAL/PERIPHERAL DISTRIBUTION	Central	0(0%)	1(2.08%)	2.3 (0.02 - 243.92)	0.7264			
	Peripheral	25(49.02%)	36(75%)		.			
	No predominance	11(21.57%)	11(22.92%)	0.7 (0.26 - 1.86)	0.4728			
	Patchy	15(29.41%)	0(0%)	0.02 (0 - 0.43)	0.0118*			
UPPER ZONE								
CONSOLIDATION								
PRESENCE	No	24(47.06%)	42(87.5%)		.			
	Yes	27(52.94%)	6(12.5%)	0.14 (0.05 - 0.37)	<.0001*		0.7 (0.62 - 0.79)	Discreta
SIDE	Absence	24(47.06%)	42(87.5%)		.			
	Unilateral	4(7.84%)	1(2.08%)	0.19 (0.02 - 1.55)	0.1210		0.7 (0.62 - 0.79)	Discreta
	Bilateral, asymmetric	15(29.41%)	3(6.25%)	0.13 (0.04 - 0.47)	0.0020*			
	Bilateral, simmetric	8(15.69%)	2(4.17%)	0.17 (0.04 - 0.81)	0.0259*			
CENTRAL/PERIPHERAL DISTRIBUTION	Absence	24(47.06%)	42(87.5%)		.			
	Central	1(1.96%)	0(0%)	0.17 (0.00 - 18.64)	0.4615		0.71 (0.63 - 0.79)	Discrete
	Peripheral	11(21.57%)	4(8.33%)	0.23 (0.07 - 0.77)	0.0178*			
	No predominance	4(7.84%)	0(0%)	0.06 (0.00 - 1.74)	0.1031			
	Patchy	11(21.57%)	2(4.17%)	0.12 (0.03 - 0.56)	0.0068*			
ANTERIOR/POSTERIOR DISTRIBUTION	Absence	24(47.06%)	42(87.5%)		.			
	Anterior	2(3.92%)	3(6.25%)	0.81 (0.13 - 5.12)	0.8202		0.72 (0.64 - 0.80)	Discrete
	Posterior	17(33.33%)	1(2.08%)	0.05 (0.00 - 0.29)	0.0010*			
	No predominance	8(15.69%)	2(4.17%)	0.17 (0.04 - 0.81)	0.0259*			

AIR BRONCHOGRAM	Absence	24(47.06%)	42(87.5%)		.			
	Always present	1(1.96%)	2(4.17%)	0.96 (0.09 - 10.50)	0.9740		0.72 (0.64 - 0.80)	Discrete
	Not always present	14(27.45%)	4(8.33%)	0.18 (0.05 - 0.59)	0.0048*			
	Never present	12(23.53%)	0(0%)	0.023 (0.00 - 0.46)	0.0133*			
ORGANISING PENUMONIA	Absence	24(47.06%)	42(87.5%)		.			
	No	14(27.45%)	5(10.42%)	0.22 (0.07 - 0.67)	0.0081*		0.71 (0.63 - 0.8)	Discreta
	Yes	13(25.49%)	1(2.08%)	0.06 (0.01 - 0.39)	0.0030*			
FIBROSIS	No consolidations	24(47.06%)	42(87.5%)		.			
	No	24(47.06%)	2(4.17%)	0.06 (0.01 - 0.24)	<.0001*		0.72 (0.64 - 0.80)	Discrete
	Yes	3(5.88%)	4(8.33%)	0.74 (0.15 - 3.58)	0.7092			
GGO								
PRESENCE	No	8(15.69%)	12(25%)		.			
	Yes	43(84.31%)	36(75%)	0.57 (0.21 - 1.55)	0.2698			
SIDE	Absence	8(15.69%)	12(25%)		.			
	Unilateral	6(11.76%)	3(6.25%)	0.37 (0.07 - 1.88)	0.2285		0.64 (0.54 - 0.75)	Scarce
	Bilateral, asymmetric	20(39.22%)	8(16.67%)	0.28 (0.08 - 0.94)	0.0400*			
	Bilateral, symmetric	17(33.33%)	25(52.08%)	0.99 (0.33 - 2.93)	0.9868			
PATTERN	Absence	8(15.69%)	12(25%)	2.23 (0.72 - 6.93)	0.1646		0.78 (0.69 - 0.87)	Discreta
	(Multi)focal	17(33.33%)	1(2.08%)	0.13 (0.02 - 0.83)	0.0307*			
	Diffuse	6(11.76%)	22(45.83%)	5.26 (1.7 - 16.26)	0.0040*			
	Both	20(39.22%)	13(27.08%)		.			
ANTERIOR/POSTERIOR DISTRIBUTION	Absence	8(15.69%)	12(25%)		.			
	Anterior	3(5.88%)	4(8.33%)	0.87 (0.15 - 4.98)	0.8796			
	Posterior	19(37.25%)	11(22.92%)	0.40 (0.13 - 1.28)	0.1227			
	No predominance	21(41.18%)	21(43.75%)	0.68 (0.23 – 2.00)	0.4834			
ROUNDED	Absence	8(15.69%)	12(25%)	4.41 (1.44 - 13.51)	0.0093*		0.74 (0.64 - 0.83)	Discreta

	Rounded	34(66.67%)	11(22.92%)		.			
	Not rounded	9(17.65%)	25(52.08%)	8.05 (2.92 - 22.18)	<.0001*			
FIBROSIS IN FOCAL LESIONS	Absence	14(27.45%)	34(70.83%)		.			
	No	37(72.55%)	6(12.5%)	0.07 (0.03 - 0.21)	<.0001*		0.82 (0.75 - 0.90)	Good
	Yes	0(0%)	8(16.67%)	7.15 (0.33 - 156.76)	0.2120			
FIBROSIS	No GGO	8(15.69%)	12(25%)		.			
	No	39(76.47%)	19(39.58%)	0.336 (0.118 - 0.957)	0.0410		0.702 (0.61 - 0.795)	Discreta
	Yes	4(7.84%)	17(35.42%)	2.644 (0.661 - 10.575)	0.1692			
CRAZY PAVING								
PRESENCE	No	40(78.43%)	45(93.75%)		.			
	Yes	11(21.57%)	3(6.25%)	0.27 (0.07 - 1.00)	0.0507			
SIDE	Absence	40(78.43%)	45(93.75%)		.			
	Unilateral	1(1.96%)	0(0%)	0.27 (0.00 - 28.38)	0.5837			
	Bilateral, asymmetric	8(15.69%)	1(2.08%)	0.16 (0.02 - 1.03)	0.0535			
	Bilateral, symmetric	2(3.92%)	2(4.17%)	0.89 (0.12 - 6.61)	0.9094			
CENTRAL/PERIPHERAL CP DISTRIBUTION	Absence	40(78.43%)	45(93.75%)		.			
	Mostly peripheral	3(5.88%)	1(2.08%)	0.38 (0.04 - 3.38)	0.3864			
	No predominance	5(9.8%)	1(2.08%)	0.243 (0.033 - 1.79)	0.1645			
	Patchy	3(5.88%)	1(2.08%)	0.382 (0.04 - 3.38)	0.3864			
	central	0(0%)	0(0%)					
ANTERIOR/POSTERIOR DISTRIBUTION	Absence	40(78.43%)	45(93.75%)		.			
	Anterior	1(1.96%)	1(2.08%)	0.89 (0.05 - 14.71)	0.9354			
	Posterior	3(5.88%)	0(0%)	0.13 (0.00 -4.00)	0.2411			
	No predominance	7(13.73%)	2(4.17%)	0.30 (0.06 - 1.42)	0.1288			
RETICULATIONS								
PRESENCE	No	48(94.12%)	19(39.58%)		.			

	Yes	3(5.88%)	29(60.42%)	20.97 (6.05 - 72.73)	<.0001*		0.77 (0.70 - 0.85)	Discrete
SIDE	Absence	48(94.12%)	19(39.58%)		.			
	Bilateral, asymmetric	2(3.92%)	5(10.42%)	5.47 (1.02 - 29.45)	0.0479*		0.78 (0.70 - 0.86)	Discrete
	bilateral, symmetric	1(1.96%)	24(50%)	40.62 (6.97 - 236.73)	<.0001*			
CENTRAL/PERIPHERAL DISTRIBUTION	Absence	48(94.12%)	19(39.58%)		.			
	Central	0(0%)	1(2.08%)	8.06 (0.08 - 841.59)	0.3787		0.77 (0.69 - 0.85)	Discrete
	Peripheral	3(5.88%)	26(54.17%)	18.83 (5.39 - 65.81)	<.0001*			
	No predominance	0(0%)	2(4.17%)	12.44 (0.29 - 532.11)	0.1884			
	patchy	0(0%)	0(0%)					
ANTERIOR/POSTERIOR DISTRIBUTION	Absence	48(94.12%)	19(39.58%)		.			
	Anterior	0(0%)	7(14.58%)	37.31 (1.67 - 833.35)	0.0224*		0.78 (0.71 - 0.86)	Discrete
	Posterior	3(5.88%)	9(18.75%)	6.75 (1.70 - 26.86)	0.0067*			
	No predominance	0(0%)	13(27.08%)	67.14 (3.42 - 1317.13)	0.0056*			
SIGNS OF FIBROSIS INSIDE RET	Absence	48(94.12%)	20(41.67%)		.			
	No	2(3.92%)	3(6.25%)	3.31 (0.52 - 21.12)	0.2051		0.77 (0.69 - 0.85)	Discrete
	Yes	1(1.96%)	25(52.08%)	40.22 (6.94 - 233.02)	<.0001*			
HONEY COMBING								
PRESENCE	No	50(98.04%)	42(87.5%)		.			
	Yes	1(1.96%)	6(12.5%)	5.15 (0.74 - 35.86)	0.0982			
SIDE	Absence	50(98.04%)	43(89.58%)		.			
	Bilateral, symmetric	1(1.96%)	5(10.42%)	4.26 (0.58 - 31.20)	0.1542			
	Bilateral asymmetric	0(0%)	0(0%)					
CENTRAL/PERIPHERAL DISTRIBUTION	Absence	50(98.04%)	42(87.5%)		.			
	Peripheral	1(1.96%)	5(10.42%)	4.36 (0.59 - 31.96)	0.1477			
	Central	0(0%)	0(0%)					
	No predominance	0(0%)	1(2.08%)	3.77 (0.04 - 379.86)	0.5723			

ANTERIOR/POSTERIOR DISTRIBUTION	Absence	50(98.04%)	42(87.5%)		.			
	Anterior	0(0%)	2(4.17%)	5.94 (0.14 - 250.44)	0.3506			
	Posterior	0(0%)	1(2.08%)	3.85 (0.04 - 396.50)	0.5687			
	No predominance	1(1.96%)	3(6.25%)	2.77 (0.31 - 24.46)	0.3587			
	Patchy	0(0%)	0(0%)					
VESSEL TICKENING	Absence	7(13.73%)	5(10.42%)	0.49 (0.14 - 1.7)	0.2623		0.68 (0.6 - 0.76)	Scarse
	No	28(54.9%)	42(87.5%)		.			
	Yes	16(31.37%)	1(2.08%)	0.06 (0.01 - 0.36)	0.0021*			
SUBPLEURAL LINES	No	38(74.51%)	42(87.5%)		.			
	Yes	13(25.49%)	6(12.5%)	0.44 (0.15 - 1.25)	0.1235			
LOWER ZONE								
CONSOLIDATION								
PRESENCE	No	8(15.69%)	44(91.67%)		.			
	Yes	43(84.31%)	4(8.33%)	0.02 (0.00 - 0.07)	<.0001*		0.88 (0.82 - 0.94)	Good
SIDE	Absence	8(15.69%)	44(91.67%)		.			
	Unilateral	10(19.61%)	3(6.25%)	0.06 (0.01 - 0.27)	0.0002*		0.90 (0.84 - 0.96)	Exellent
	Bilateral, asymmetrical	16(31.37%)	0(0%)	0.01 (0 - 0.11)	0.0007*			
	Bilateral, simmetric	17(33.33%)	1(2.08%)	0.02(0.00 - 0.11)	<.0001*			
CENTRAL/PERIPHERAL DISTRIBUTION	Absence	8(15.69%)	44(91.67%)		.			
	mostly central	1(1.96%)	0(0%)	0.06 (0.00 - 6.24)	0.2402		0.89 (0.82 - 0.95)	Good
	Peripheral	32(62.75%)	3(6.25%)	0.02 (0.00 - 0.08)	<.0001*			
	No predominance	5(9.8%)	0(0%)	0.02 (0.00 - 0.45)	0.0147*			
	Patchy	5(9.8%)	1(2.08%)	0.05 (0.01 - 0.42)	0.0055*			
ANTERIOR/POSTERIOR DISTRIBUTION	Absence	8(15.69%)	44(91.67%)		.			
	Anterior	4(7.84%)	0(0%)	0.02 (0.00 - 0.60)	0.0242*		0.88 (0.82 - 0.95)	Good

	Posterior	33(64.71%)	3(6.25%)	0.02 (0.00 - 0.08)	<.0001*			
	No predominance	6(11.76%)	1(2.08%)	0.04 (0.01 - 0.34)	0.0027*			
AIR BRONCHOGRAM	Absence	8(15.69%)	44(91.67%)	REF	.		0.89 (0.82 - 0.95)	Good
	Not always present	18(35.29%)	1(2.08%)	0.015 (0.00 - 0.1)	<.0001*			
	Always present	0(0%)	0(0%)					
	Never present	25(49.02%)	3(6.25%)	0.03 (0.01 - 0.10)	<.0001*			
ORGANISING PNEUMONIA	Absence	8(15.69%)	44(91.67%)		.			
	No	18(35.29%)	2(4.17%)	0.026 (0.01 - 0.12)	<.0001*		0.88 (0.82 - 0.95)	good
	Yes	25(49.02%)	2(4.17%)	0.02 (0.00 - 0.08)	<.0001*			
FIBROSIS	Absence	8(15.69%)	44(91.67%)		.			
	No	34(66.67%)	1(2.08%)	0.1(0.00 - 0.05)	<.0001*		0.90 (0.84 - 0.96)	good
	Yes	9(17.65%)	3(6.25%)	0.07 (0.02 - 0.31)	0.0004*			
GGO								
PRESENCE OF GGO	No	5(9.8%)	4(8.33%)		.			
	Yes	46(90.2%)	44(91.67%)	1.17 (0.29 - 4.63)	0.8233			
SIDE	Absence	5(9.8%)	4(8.33%)		.			
	Unilateral	4(7.84%)	0(0%)	0.13 (0.00 - 4.59)	0.2664			
	bilateral, asymmetric	26(50.98%)	5(10.42%)	0.25 (0.05 - 1.27)	0.0951			
	bilateral, symmetric	16(31.37%)	39(81.25%)	2.93 (0.70 - 12.29)	0.1427			
PATTERN	Absence	5(9.8%)	4(8.33%)		.			
	(Multi)focal	13(25.49%)	1(2.08%)	0.14 (0.01 - 1.21)	0.0733		0.84 (0.76 - 0.91)	good
	diffuse	4(7.84%)	32(66.67%)	8.83 (1.69 - 45.97)	0.0097*			
	Both	29(56.86%)	11(22.92%)	0.48 (0.11 - 2.1)	0.3273			
ANTERIOR/POSTERIOR DISTRIBUTION	Absence	5(9.8%)	4(8.33%)		.			
	Anterior	3(5.88%)	0(0%)	0.17 (0.00 - 6.82)	0.3506			
	Posterior	26(50.98%)	20(41.67%)	0.94 (0.22 - 3.98)	0.9391			

	No predominance	17(33.33%)	24(50%)	1.71 (0.4 - 7.31)	0.4686			
ROUNDED GGO	Absence	5(9.8%)	4(8.33%)	3.32 (0.74 - 14.81)	0.1165		0.81 (0.73 - 0.89)	Good
	Rounded	38(74.51%)	9(18.75%)		.			
	Non rounded	8(15.69%)	35(72.92%)	16.93 (5.96 - 48.04)	<.0001*			
FIBROSIS INSIDE FOCAL ALTERATIONS	No GGO	5(9.8%)	4(8.33%)	7.73 (1.5 - 39.83)	0.0145*		0.91 (0.85 - 0.97)	Exellent
	No	42(82.35%)	4(8.33%)		.			
	Yes	4(7.84%)	40(83.33%)	85.01 (21.15 - 341.6)	<.0001*			
FIBROSIS	Absence	5(9.8%)	4(8.33%)		.			
	No	42(82.35%)	4(8.33%)	0.129 (0.025 - 0.667)	0.0145		0.908 (0.849 - 0.967)	Exellent
	Yes	4(7.84%)	40(83.33%)	11 (2.131 - 56.794)	0.0042			
CRAZY PAVING								
PRESENCE	No	38(74.51%)	43(89.58%)		.			
	Yes	13(25.49%)	5(10.42%)	0.36 (0.12 - 1.09)	0.0712			
SIDE	Absence	38(74.51%)	43(89.58%)		.			
	Unilateral	3(5.88%)	0(0%)	0.13 (0.00 - 3.98)	0.2399			
	Bilateral, asymmetric	3(5.88%)	0(0%)	0.13 (0.00 - 3.98)	0.2399			
	bilateral, symmetric	7(13.73%)	5(10.42%)	0.65 (0.19 - 2.21)	0.4894			
CENTRAL/PERIPHERAL CP DISTRIBUTION	Absence	38(74.51%)	43(89.58%)		.			
	Central	1(1.96%)	1(2.08%)	0.88 (0.05 - 14.64)	0.9320			
	Peripheral	6(11.76%)	4(8.33%)	0.613 (0.16 - 2.33)	0.4717			
	No predominance	4(7.84%)	0(0%)	0.10 (0.00 - 2.65)	0.1678			
	Patchy	2(3.92%)	0(0%)	0.18 (0.00 - 7.48)	0.3648			
ANTERIOR/POSTERIOR DISTRIBUTION	Absence	38(74.51%)	43(89.58%)		.			
	Anterior	1(1.96%)	1(2.08%)	0.89 (0.05 - 14.65)	0.9323			
	Posterior	7(13.73%)	2(4.17%)	0.3 (0.06 - 1.42)	0.1277			
	No predomiannce	5(9.8%)	2(4.17%)	0.4 (0.08 - 2.11)	0.2814			

RETICULATIONS								
PRESENCE	No	49(96.08%)	7(14.58%)		.			
	Yes	2(3.92%)	41(85.42%)	109.59 (24.31 - 494.08)	<.0001*		0.91 (0.85 - 0.96)	Exellent
SIDE	Absence	49(96.08%)	7(14.58%)		.			
	bilateral asymmetric	0(0%)	2(4.17%)	33.02 (0.74 - 1474.71)	0.0712		0.91 (0.85 - 0.96)	Exellent
	Monolateral	0(0%)	0(0%)					
	bilateral symmetric	2(3.92%)	39(81.25%)	104.28 (23.08 - 471.10)	<.0001*			
CENTRAL/PERIPHERAL RET DISTRIBUTION	Absence	49(96.08%)	7(14.58%)		.			
	Central	0(0%)	4(8.33%)	59.37 (2.07 - 1703.46)	0.0171*		0.91 (0.85 - 0.96)	Exellent
	Peripheral	2(3.92%)	30(62.5%)	80.52 (17.58 - 368.69)	<.0001*			
	No predominance	0(0%)	7(14.58%)	99.02 (4.21 - 2327.31)	0.0043*			
ANTERIOR/POSTERIOR DISTRIBUTION	Absence	49(96.08%)	7(14.58%)		.			
	Anterior	0(0%)	1(2.08%)	21.77 (0.20 - 2400.98)	0.1992		0.92 (0.86 - 0.97)	Exellent
	Posterior	2(3.92%)	19(39.58%)	51.48 (10.88 - 243.64)	<.0001*			
	No predominance	0(0%)	21(43.75%)	283.80 (14.52 - 5546.13)	0.0002*			
FIBROSIS	Absence	49(96.08%)	7(14.58%)		.			
	No	1(1.96%)	2(4.17%)	11 (0.94 - 129.11)	0.0563		0.92 (0.86 - 0.97)	Exellent
	Yes	1(1.96%)	39(81.25%)	173.8 (28.06 - 1076.39)	<.0001*			
HONEYCOMBING								
PRESENCE	No	51(100%)	34(70.83%)		.			
	Yes	0(0%)	14(29.17%)	43.28 (2.26 - 826.89)	0.0123*		0.65 (0.58 - 0.71)	Scarce
SIDE	Absence	51(100%)	34(70.83%)		.			
	Unilateral	0(0%)	1(2.08%)	4.83 (0.05 - 498.51)	0.5054		0.65 (0.58 - 0.71)	Scarce
	Bilateral, asymmetric	0(0%)	3(6.25%)	10.45 (0.33 - 328.82)	0.1824			
	Bilateral, symmetric	0(0%)	10(20.83%)	31.35 (1.55 - 634.03)	0.0247*			
CENTRAL/PERIPHER	Absence	51(100%)	34(70.83%)		.			

AL DISTRIBUTION	Central	0(0%)	0(0%)					
	Peripheral	0(0%)	11(22.92%)	34.33 (1.73 - 682.05)	0.0204*		0.646 (0.58 - 0.71)	Scarce
	No predominance	0(0%)	3(6.25%)	10.45 (0.33 - 328.57)	0.1824			
ANTERIOR/POSTERIOR DISTRIBUTION	Absence	51(100%)	34(70.83%)		.			
	Anterior	0(0%)	0(0%)					
	Posterior	0(0%)	10(20.83%)	31.35 (1.55 - 633.95)	0.0247*		0.65 (0.58 - 0.71)	Scarce
	No predominance	0(0%)	4(8.33%)	13.43 (0.50 - 362.13)	0.1223			
VESSEL TICKENING	Absence	5(9.8%)	0(0%)	0.05 (0 - 1.33)	0.0740		0.72 (0.64 - 0.79)	Discreta
	No	27(52.94%)	46(95.83%)		.			
	Yes	19(37.25%)	2(4.17%)	0.08 (0.02 - 0.32)	0.0004*			
SUBPLEURAL LINES	No	33(64.71%)	37(77.08%)		.			
	Yes	18(35.29%)	11(22.92%)	0.55 (0.23 - 1.34)	0.1921			
PLEURAL AND MEDIASTINAL INVOLVMENT								
PERICARDIAL EFFUSION	No	47(92.16%)	38(79.17%)		.			
	Yes	4(7.84%)	10(20.83%)	2.88 (0.85 - 9.76)	0.0895			
PLEURAL EFFUSION	No	39(76.47%)	45(93.75%)		.			
	Yes, unilateral	6(11.76%)	2(4.17%)	0.33 (0.07 - 1.66)	0.1805			
	Yes, bilateral	6(11.76%)	1(2.08%)	0.2 (0.03 - 1.40)	0.1053			
PLEURAL RETRACTION	No	51(100%)	38(79.17%)		.			
	Yes	0(0%)	10(20.83%)	28.11 (1.39 - 567.79)	0.0296*		0.60 (0.55 - 0.66)	Scarse
PLEURAL THIKENING	No	26(50.98%)	34(70.83%)		.			
	Yes	25(49.02%)	14(29.17%)	0.44 (0.19 - 1)	0.0501			
LYNPHADENOPATHY	No	36(70.59%)	29(60.42%)		.			
	Yes	15(29.41%)	19(39.58%)	1.56 (0.67 - 3.59)	0.2992			
DILATED ESOPHAGOUS	No	43(84.31%)	8(16.67%)		.			
	Yes	8(15.69%)	40(83.33%)	24.38 (8.51 - 69.90)	<.0001*		0.84 (0.76 - 0.91)	Good

SCORES								
CO-RADS	0	0(0%)	1(2.08%)		.			
	1	3(5.88%)	33(68.75%)	3.19 (0.03 - 337.71)	0.6260			
	2	14(27.45%)	2(4.17%)	0.06 (0.00 - 6.53)	0.2368			
	3	11(21.57%)	8(16.67%)	0.25 (0.00 - 24.93)	0.5519			
	4	14(27.45%)	4(8.33%)	0.10 (0.00 - 10.87)	0.3394			
	5	9(17.65%)	0(0%)	0.02 (0 -4.00)	0.1444			
COVID-19 (RSNA)	typical	28(54.9%)	2(4.17%)		.			
	indeterminate	17(33.33%)	7(14.58%)	4.89 (1.01 - 23.67)	0.0488		0.88 (0.81 - 0.95)	good
	atypical	6(11.76%)	39(81.25%)	69.28 (14.57 - 329.41)	<.0001			

Legend:

*P<0.05

GGO: Ground glass opacities; Absence: absence of the alteration for which the subanalysis should have been performed

Supplementary Data S1. Background of the readers.

RAD	Practice location	Number of years in practice	Radiological Specialization	Training specific for Imaging in Rheumatic Disease	Training for COVID-19 infection
1	Treviso (Italy)	7	Chest-RAD	MDT	Real-life cases
2	Florence (Italy)	20	Chest-RAD	Real life cases	Real-life cases
3	Florence (Italy)	10	n-chest-RAD	Real life cases	Real-life cases
4	Catania (Italy)	10	Chest-RAD	Real life cases	Real-life cases
5	Milan (Italy)	20	n-chest-RAD	Real life cases	Real-life cases
6	Siena (Italy)	15	Chest-RAD	Real life cases	Real-life cases
7	Vercelli (Italy)	15	n-chest-RAD	Real life cases	Real-life cases
nRAD			**Medical Specialization**	**Training in Imaging in Rheumatic disease**	
1	Florence (Italy)	5-10	Rheumatologist	Real life -cases	scientific literature
2	Florence (Italy)	10-15	Rheumatologist	Real-life cases	scientific literature
3	Florence (Italy)	10-15	Rheumatologist	Real-life cases	scientific literature
4	London (UK)	20	Rheumatologist	Real-life cases	scientific literature
5	Sheffield (UK)	14	Rheumatologist	Real-life cases	Real-life cases
6	Trieste (Italy)	10	Rheumatologist	Real life cases	Real life cases
7	Florence (Italy)	5-10	Infectious and Tropical Diseases	scientific literature	Real-life cases
8	Florence (Italy)	5-10	Infectious and Tropical Diseases	scientific literature	Real-life cases
9	Catania (Italy)	5-10	Immunologist	Real-life cases	Real-life cases
10	Naples (Italy)	20	Immunologist	Real-life cases	scientific literature
11	Milan (Italy)	5-10	Rheumatologist	Real-life cases	Real-life cases
12	Catania (Italy)	20	Pulmonologist	MDT	Real-life cases
13	Milan (Italy)	20	Pulmonologist	MDT	Real-life cases
14	Florence (Italy)	15	Pulmonologist	MDT	Real-life cases
15	Milan (Italy)	20	Pulmonologist	MDT	Real-life cases

Legend.

MDT: multidisciplinary team; RAD: radiologist group; nRad: non-radiologist group; Chest-RAD: chest radiologists, with at least more than 5 years of experience; n-chest-RAD: radiologists without chest experience.

Supplementary Data S2. Definition of all CT lesions and anatomical references.

The following lesions were defined in according to the radiological guideline of the Fleischer Society [1]:

- **Consolidation (CONS)** is defined as homogeneous increase in pulmonary parenchymal attenuation that obscures the margins of vessels and airway walls;
- **Organizing Pneumonia (OP)** is defined as airspace consolidation, typically subpleural, sometimes broncho-centric;
- **Ground glass opacity (GGO)** is represented by hazy increased opacity of lung, with preservation of bronchial and vascular margins;
- **Reticulations (RET)** are septal thickenings that, by summation, produce an appearance resembling a net;
- **Crazy paving (CP)** is defined as thickened interlobular septa and intralobular lines superimposed on a background of ground-glass opacity;
- **Honey combing (HC)** is defined as clustered cystic air spaces, typically of comparable diameters, on the order of 3–10, mm but occasionally as large as 2.5 cm;
- **subpleural lines** are curvilinear opacity, 1–3 mm in thickness, lying less than 1 cm from and parallel to the pleural surface; lymphadenopathy is mediastinal nodes with short-axis diameter > 1 cm;
- **architectural distortion** are abnormal displacement of bronchi, vessels, fissures or septa;
- **Bronchiectasis** are identified by bronchial dilatation with respect to the accompanying pulmonary artery, lack of tapering of bronchi and identification of bronchi within 1 cm of the pleural surface.

Moreover, we defined a **dilated esophagus** when the inner air-filled diameter was > 1cm [2]; **vessel thickening inside alterations** as vessel diameter larger than in comparable regions of non-diseased lung, or focal dilation or non-tapering of vessels as they course toward the lung periphery [3]; **pleural thickening** as increase in soft tissue at the lung-pleural interface [4].

The carina was adopted as anatomical landmark for upper and lower zones as well as for anterior and posterior location. We defined “peripheral lung” as two or three rows of secondary pulmonary lobules, forming a layer of three to four centimetres in thickness at the lung periphery, the central lung accounts for the remaining parts, adopting the definition reported by Nishino et al. [5]

Patterns were defined as follows:

- Focal pattern: presence of nodule(s) or mass(es), following the definitions of the Fleischner society [1]. However, a lung mass needs to show well defined shape, namely rounded or oval, to be considered as focal lesion.

- **Diffuse pattern**: presence of alterations that don't meet the definition of neither nodule nor mass, following the definitions of the Fleischner society [1]. However, masses with polygonal shapes were considered as manifestation of diffuse disease.

- **(Multi)Focal and diffuse pattern**: coexistence of both patterns (Figure 1)

For disease pattern, that consider the whole lungs field, we also adopt the term white lung, when the sum of all alterations covered almost the totality of lung parenchyma (>90%), making impossible to define if the global aspect was due to the coalescence of multifocal lesions, to an extended diffuse disease, or both.

1. Hansell DM, Bankier AA, MacMahon H, McLoud TC, Müller NL, Remy J. Fleischner Society: glossary of terms for thoracic imaging. Radiology. 2008;246(3):697-722.

2. Schraufnagel DE, Michel JC, Sheppard TJ, Saffold PC, Kondos GT. CT of the normal esophagus to define the normal air column and its extent and distribution. AJR Am J Roentgenol. 2008 Sep;191(3):748-52. doi: 10.2214/AJR.07.3455. PMID: 18716104.

3. Min Lang, Avik Som, Denston Carey, et al. Pulmonary Vascular Manifestations of COVID-19 Pneumonia. Little Radiology: Cardiothoracic Imaging 2020 2:3.

4. Hallifax RJ, Talwar A, Wrightson JM, et al. State-of-the-art: Radiological investigation of pleural disease. Respir Med. 2017 Mar;124:88-99.

5. Nishino M, Itoh H, Hatabu H. A practical approach to high-resolution CT of diffuse lung disease. *Eur J Radiol*. 2014;83(1):6-19.